

# Signal Propagation in Nonlinear Stochastic Gene Regulatory Networks

Sever Achimescu<sup>1,\*</sup> and Ovidiu Lipan<sup>1,†</sup>

<sup>1</sup>*Center for Biotechnology and Genomic Medicine  
Medical College of Georgia,  
1120m 15th St., Ca-4124, Augusta, GA 30912  
(Dated: May 18, 2005)*

**The structure of a stochastic nonlinear gene regulatory network is uncovered by studying its response to input signal generators. Four applications are studied in detail: a nonlinear connection of two linear systems, the design of a logic pulse, a molecular amplifier and the interference of three signal generators in E2F1 regulatory element. The gene interactions are presented using molecular diagrams that have a precise mathematical structure and retain the biological meaning of the processes.**

Excerpts from this manuscript were presented at the 3rd International Conference on Pathways, Networks, and Systems: Theory and Experiments, October 2-7, Rhodes Greece 2005, [1].

## I. INTRODUCTION

A living organism is a complex interconnection of many control units that form a gene regulatory network. In developmental biology, clusters of DNA sequence elements (cis-regulatory module) are target sites for transcription factors. One cis-regulatory module controls a set of gene expression both in space (location) and time [2]. One transcription factor can interact with many modules, and one module is controlled by many transcription factors. Thus, the time and space variation of a gene expression is a consequence of an interconnected network of interactions.

With the advent of high throughput technologies (microarrays, proteomics tools) the need for quantitative models of gene networks becomes a reality [3, 4, 5]. In recent years we have witnessed a growing interest in experiments within the field of systems biology that require mathematical models to describe the experimental results [6, 7, 8, 9, 10, 11, 12]. A mathematical model for gene regulatory networks is also closely related with synthetic biology, the engineering counterpart of systems biology [13, 14, 15]. Similar with the development of the field of electronics, where complex equipment is built on interconnected simple devices, the field of synthetic biology aims to build simple molecular devices for later use in more complex molecular machines [16, 17]. To build a robust, reliable, and simple device, the molecular engineer needs to have a mathematical description of the system in order to evaluate the number, range and meaning of a group of parameters that are critical for the device functionality. As with any mathematical model of a natural system, the models of a gene regulatory network must fulfill certain constraints. At present, the community of researchers agrees that a gene regulation model must be nonlinear and stochastic. Nonlinearity is a widespread phenomena in life science [18, 19]. When two molecules dimerize to form a complex, the concentration of the complex is proportional to the product of the concentrations of the molecules involved

---

\*Electronic address: sachimescu@mcg.edu

†Electronic address: olipan@mcg.edu

To whom correspondence should be addressed: olipan@mcg.edu

in the process. Multimerization will require polynomial functions in molecular concentrations [20]; furthermore, rational functions are used to model the most simple gene autoregulatory system [21]. The model should be also stochastic, its molecules being subjected to the thermodynamics laws of fluctuation. Two cell lines with identical genetic background can show variation in phenotype due only to a probabilistic distribution of the molecule number inside the cell [22]. The stochastic process that describe molecular interactions are fundamentally discrete; the molecule number can change by an integer amount only. Fluctuations in biological systems created by these stochastic processes, are described by a Master Equation [20]. Approximations to the Master Equation, like the Fokker-Planck, Langevin and  $\Omega$  expansion, are often use [23, 24, 25, 26]. However, many biological regulatory systems function with molecules present in low numbers [27]. For such systems, the Master Equation should not be approximated [28, 29, 30, 31]. Another requirement for the model is to explain the flow of a signal as it passes through the genetic network. To reveal the structure of a gene regulatory interactions, input signals (growth factors, heat shocks, drugs) are inserted into different positions within a gene regulatory network. Then, output signals are measured at some other positions. A coherent model of the network must explain the measured input-output relations and must provide predictions that can be experimentally tested. It is desirable to know how measured data is related with the input signal [4, 30, 32]. In engineering sciences [33], control theory explains in mathematical terms the relation between the input and output signals (measured data). The same theory provides ways to design stable systems using feedback signals. Ideas from Control Theory translated into molecular biology will help the design process in synthetic biology.

In [30] it is proposed that signal generators controlled by light, [34], should be incorporated into the gene regulatory network. With the help of these light-controlled signal generators, different types of signal perturbations can be imposed on the gene regulatory network. In [30] the Master Equation was solved for systems that are linear in the transition probabilities. The network's response to signal generators was expressed in terms of a transfer matrix for the first and second order moments of the stochastic process. Our goal in this article is to construct a mathematical description of a gene regulatory network that is nonlinear, stochastic and explains the input-output relations as in control theory. The nonlinearity means that the transition probabilities are rational functions in the molecule numbers. We do not use Fokker-Planck, Langevin or  $\Omega$  expansion to approximate the Master Equation. For polynomial transition probabilities, the time evolution equation for the factorial cumulants will have the following form:

$$\dot{X}_{\alpha_1\alpha_2\dots\alpha_n} = \left\{ R_{\alpha_1\alpha_2\dots\alpha_k}^m(t) \sum_{Y,\sigma} X_{\alpha_{k+1}|\dots|\alpha_n|Y[m^\sigma]} \right\}_\alpha \quad (\text{I.1})$$

If the transition probabilities are rational functions, the equations are (III.54). The signal generators are part of the coefficients  $R_{\alpha_1\alpha_2\dots\alpha_k}^m(t)$ . Before the theory is presented, we will solve four genetic regulatory networks to explain all the notations and meaning of the variables in (I.1) and (III.54). The examples are also meant to provide practical applications of the underlying theory.

## II. RESULTS

### A. Two Genes Coupled by a Nonlinear Interaction

The aim of this subsection is twofold: to introduce the notations that will later be generalized, and to explain how the classical control theory model changes due to stochastic effects. Each genetic regulatory network is built on a set of interacting molecular species. In the present case the entire

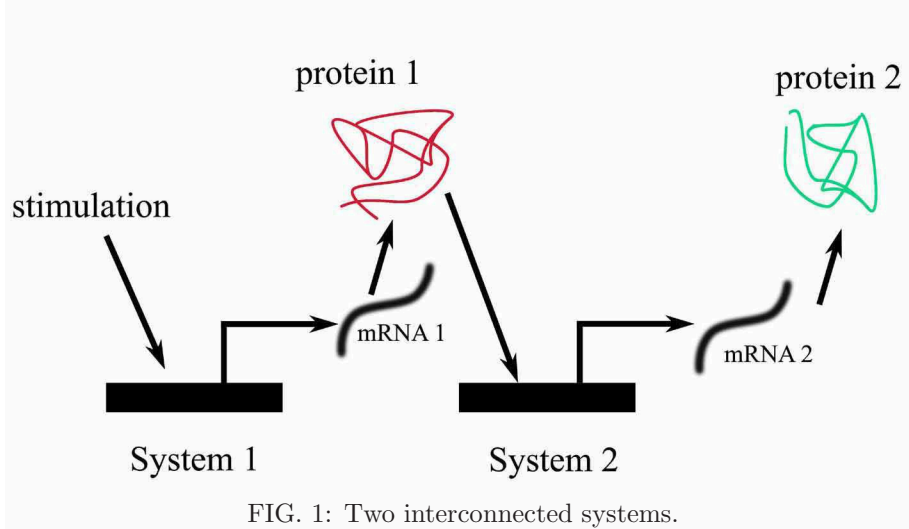


FIG. 1: Two interconnected systems.

network is composed of System 1, with mRNA1 and protein1 as molecular species, coupled with System 2 with mRNA2 and protein2 as its molecular species. The number of mRNA1 is denoted by  $r_1$  and similar notations for the other three components. At a given time, the *state* of the network will be denoted by

$$q \equiv (q_1, q_2, q_3, q_4) = (r_1, p_1, r_2, p_2). \quad (\text{II.1})$$

The mRNA1 is controlled by an input generator and thus the state  $q$  will evolve in time. Such a generator can be practically constructed using a yeast two-hybrid system, as is described in [34]. The light-switch is based on phytochrome that is synthesized in darkness in the Q1 form, Fig. 2. A red light photon of wavelength 664 nm shined on the Q1 form of the protein transforms it in the form Q2. Fig. 2 presents the state of the switch after the effect of the corresponding wavelength took place. When Q2 absorbs a far red light of wavelength 748 nm, the molecule Q goes back to its original form, Q1. These transitions take milliseconds. The protein P interacts only with the Q2 form, recruiting thus the activation domain to the target promoter. In this position, the promoter is open and the gene is transcribed. After the desired time elapsed, the gene can be turned off by a photon from a far red light source. Using a sequence of red and far red light pulses the molecular switch can be opened and closed.

The time evolution of the *state* depends on all possible *transitions* that can appear in the system. For example, from the state  $(r_1, p_1, r_2, p_2)$  at time  $t$ , the system can move to the state with one more protein1 molecule  $(r_1, p_1 + 1, r_2, p_2)$  because mRNA1 is translated. This transition is described by a vector  $\epsilon_2 = (0, 1, 0, 0)$  that shows the change in the state:  $(r_1, p_1 + 1, r_2, p_2) = (r_1, p_1, r_2, p_2) + \epsilon_2$ . The list of all possible transitions is described in the first column of Table 1. Which transition will actually take place is governed by a stochastic process [20]. A third element in the model (beside the *state* and *transitions*) is the set of all transition probabilities  $T_\epsilon$ . If the state at time  $t$  is  $q$ , then the probability of the system to jump in the state  $q + \epsilon$  at the time  $t + dt$  is  $T_\epsilon(q, t)dt$ . The presence of the time  $t$  in the argument of the transition function show that, in general, the transition depends not only on the number of molecules in the system, but also on the moment in time when it is recorded.  $T_{\epsilon_1}$  in Table 1 is a time dependent transition probability. It contains the signal generator  $G(t)$  that modulates the mRNA1 transcription.

All transition probabilities are given in the second column in Table 1. The coefficients that multiply the molecule number in a transition probability are the parameters of the model. Higher

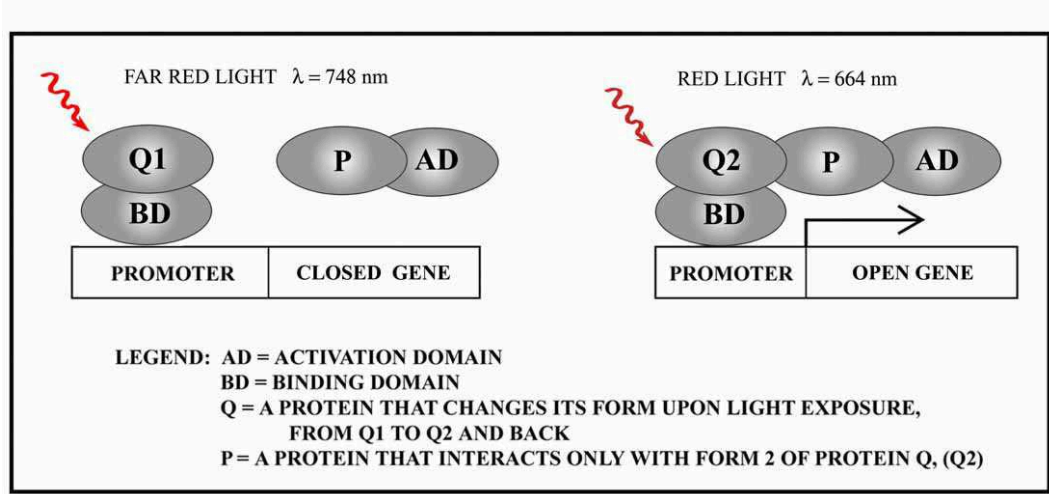


FIG. 2: Signal generator. Adapted from ref. [34].

values of the coefficient will make that transition to appear more often per unit of time. The last column of the table will be explained later in the text. The the dynamic of the genetic network is given by the time evolution of the probability of the network to be in the state  $q$  at time  $t$ :  $P(q, t)$ . The equation for the time evolution of the state probability is know as the Master Equation [20].

**TABLE 1: Nonlinear Coupling of Two Linear Systems**

	Transitions	Transition probabilities	Coefficients	Polynomial basis
Signal Generator	$\epsilon_1 = (1, 0, 0, 0)$	$T_{\epsilon_1}(q) = G(t)$	$M_{\epsilon_1}(t) = G(t)$	$\mathbf{e}_{(0,0,0,0)} = 1$
Linear System 1	$\epsilon_{-1} = (-1, 0, 0, 0)$	$T_{\epsilon_{-1}}(q) = \gamma_{r_1} r_1$	$M_{\epsilon_{-1}}^1 = \gamma_{r_1}$	$\mathbf{e}_{(1,0,0,0)} = r_1$
	$\epsilon_2 = (0, 1, 0, 0)$	$T_{\epsilon_2}(q) = k_1 r_1$	$M_{\epsilon_2}^1 = k_1$	$\mathbf{e}_{(1,0,0,0)} = r_1$
	$\epsilon_{-2} = (0, -1, 0, 0)$	$T_{\epsilon_{-2}}(q) = \gamma_{p_1} p_1$	$M_{\epsilon_{-2}}^2 = \gamma_{p_1}$	$\mathbf{e}_{(0,1,0,0)} = p_1$
Nonlinear Coupling	$\epsilon_3 = (0, 0, 1, 0)$	$T_{\epsilon_3}(q) = h p_1^2 =$ $= h p_1 (p_1 - 1) + h p_1$	$M_{\epsilon_3}^2 = h$ $M_{\epsilon_3}^{22} = h$	$\mathbf{e}_{(0,1,0,0)} = p_1$ $\mathbf{e}_{(0,2,0,0)} = p_1 (p_1 - 1)$
Linear System 2	$\epsilon_{-3} = (0, 0, -1, 0)$	$T_{\epsilon_{-3}}(q) = \gamma_{r_2} r_2$	$M_{\epsilon_{-3}}^3 = \gamma_{r_2}$	$\mathbf{e}_{(0,0,1,0)} = r_2$
	$\epsilon_4 = (0, 0, 0, 1)$	$T_{\epsilon_4}(q) = k_2 r_2$	$M_{\epsilon_4}^3 = k_2$	$\mathbf{e}_{(0,0,1,0)} = r_2$
	$\epsilon_{-4} = (0, 0, 0, -1)$	$T_{\epsilon_{-4}}(q) = \gamma_{p_2} p_2$	$M_{\epsilon_{-4}}^4 = \gamma_{p_2}$	$\mathbf{e}_{(0,0,0,1)} = p_2$

$$\begin{aligned}
P(r_1, p_1, r_2, p_2, t + dt) = & \quad (II.2) \\
& P(r_1 - 1, p_1, r_2, p_2, t) T_{\epsilon_1}(r_1 - 1, p_1, r_2, p_2, t)dt + P(r_1 + 1, p_1, r_2, p_2, t) T_{\epsilon_{-1}}(r_1 + 1, p_1, r_2, p_2, t)dt + \\
& P(r_1, p_1 - 1, r_2, p_2, t) T_{\epsilon_2}(r_1, p_1 - 1, r_2, p_2, t)dt + P(r_1, p_1 + 1, r_2, p_2, t) T_{\epsilon_{-2}}(r_1, p_1 + 1, r_2, p_2, t)dt + \\
& P(r_1, p_1, r_2 - 1, p_2, t) T_{\epsilon_3}(r_1, p_1, r_2 - 1, p_2, t)dt + P(r_1, p_1, r_2 + 1, p_2, t) T_{\epsilon_{-3}}(r_1, p_1, r_2 + 1, p_2, t)dt + \\
& P(r_1, p_1, r_2, p_2 - 1, t) T_{\epsilon_4}(r_1, p_1, r_2, p_2 - 1, t)dt + P(r_1, p_1, r_2, p_2 + 1, t) T_{\epsilon_{-4}}(r_1, p_1, r_2, p_2 + 1, t)dt + \\
& P(r_1, p_1, r_2, p_2, t) \left( 1 - T_{\epsilon_1}(r_1, p_1, r_2, p_2, t)dt - T_{\epsilon_{-1}}(r_1, p_1, r_2, p_2, t)dt - T_{\epsilon_2}(r_1, p_1, r_2, p_2, t)dt - \right. \\
& \quad T_{\epsilon_{-2}}(r_1, p_1, r_2, p_2, t)dt - T_{\epsilon_3}(r_1, p_1, r_2, p_2, t)dt - T_{\epsilon_{-3}}(r_1, p_1, r_2, p_2, t)dt - \\
& \quad \left. T_{\epsilon_4}(r_1, p_1, r_2, p_2, t)dt - T_{\epsilon_{-4}}(r_1, p_1, r_2, p_2, t)dt \right) .
\end{aligned}$$

Given that the system was at time  $t$  in the state  $q = (r_1, p_1, r_2, p_2)$ , the first 8 terms in (II.2) represent the probability that the system will be in a new state at the time  $t + dt$ . The new state depends on which transition actually took place. The rest of the terms in (II.2) express the probability that no transition will take place in  $(t, t + dt)$ . Dividing by  $dt$  and taking the limit  $dt \rightarrow 0$ , the above relation between probabilities takes the form of a partial differential equation:

$$\frac{\partial}{\partial t} P(q, t) = \sum_{\epsilon} T_{\epsilon}(q - \epsilon, t) P(q - \epsilon, t) - \sum_{\epsilon} T_{\epsilon}(q, t) P(q, t) . \quad (II.3)$$

This equation is known as the Master Equation for the jump Markov processes with discrete states [20, 35]. The summation is over all possible transitions. It is hard to solve this equation, even in very simple examples. However, we are interested in the mean number of molecules of different species and in their standard deviation. Or more generally, we want to know the correlation between different molecular species. The quantities of interest are thus means of products of state components:

$$\langle q^{\bar{m}} \rangle = \sum_q q^{\bar{m}} P(q, t) , \quad (II.4)$$

where the sum goes over all possible states. The notation  $\bar{m}$  stands for a vector  $\bar{m} = (m_1, m_2, m_3, m_4)$  of integer numbers. The number of components of  $\bar{m}$  is the same as the number of components in the state  $q$ . The power of  $q$  to the  $\bar{m}$  is defined as  $q^{\bar{m}} = q_1^{m_1} q_2^{m_2} q_3^{m_3} q_4^{m_4}$ . We need a line on top of  $m$  to distinguish it from a simple  $m$  that will be used heavily in what follows.

The time evolution for  $\langle q^{\bar{m}} \rangle$  can be obtained from the Master Equation (II.3) using the  $z$ -transform of the state probability  $P(q, t)$ :

$$F(z, t) = \mathcal{Z}(P(q, t)) \equiv \sum_q z^q P(q, t) \quad (II.5)$$

where  $z = (z_1, z_2, z_3, z_4)$  are variables in the complex plane and the power  $z^q$  was defined above. Quantities of interest are means of polynomials in the components of the state variable  $q$ , like  $\langle q^{\bar{m}} \rangle$ . A natural way to obtain means of polynomials in  $q$  is by taking derivatives with respect to  $z$  in

(II.5) and then put  $z_i = 1, i = 1 \dots 4$ . For example:

$$\langle r_1 \rangle = \frac{\partial F(z, t)}{\partial z_1} \Big|_{z=1}, \quad (\text{II.6})$$

$$\langle p_2(p_2 - 1) \rangle = \frac{\partial F(z, t)}{\partial z_4^2} \Big|_{z=1}. \quad (\text{II.7})$$

We notice that the derivatives of  $F(z, t)$  bring us to a set of polynomials that are known as decreasing factorials:

$$e_{m_k}(q_k) = q_k(q_k - 1) \dots (q_k - m_k + 1), \quad (\text{II.8})$$

$$\mathbf{e}_{\bar{m}}(q) = e_{m_1}(q_1)e_{m_2}(q_2)e_{m_3}(q_3)e_{m_4}(q_4). \quad (\text{II.9})$$

We will use the polynomials  $e_{\bar{m}}(q)$  as a base, to express all the transition probabilities, as is explained in the last column of Table 1. In this base, the results are easy to express in terms of the derivatives of  $F(z, t)$ . A decreasing factorial has a physical interpretation, [20]. In a system with  $q_k$  molecules of specie  $k$ , the probability for a collision involving  $m_k$  such molecules is proportional with  $e_{m_k}(q_k)$ . In other words, the probability for multimer formation is described by a decreasing factorial.

Every polynomial can be expressed as a linear combination of the basic polynomials  $e_{\bar{m}}(q)$ . To make a distinction between the moments  $\langle q^{\bar{m}} \rangle$  and  $\langle \mathbf{e}_{\bar{m}}(q) \rangle$ , the later one is known as a factorial moment. The first order moments (which are actually the means of the state variable) and the first order factorial moments are equal.

The variables that describe the system are thus

$$\langle \mathbf{e}_{\bar{m}}(q) \rangle = \partial_m F(z, t) \Big|_{z=1}, \quad (\text{II.10})$$

which also displays the tensor index  $m$ . From a vector index

$$\bar{m} = (m_1, m_2, m_3, m_4), \quad (\text{II.11})$$

we can construct a tensor index

$$m = \underbrace{11\dots 1}_{m_1} \underbrace{22\dots 2}_{m_2} \underbrace{33\dots 3}_{m_3} \underbrace{44\dots 4}_{m_4}, \quad (\text{II.12})$$

and vice versa. The tensor index  $m$  is useful for ordering the variables as they come from partial derivatives.

$$\partial_m = \underbrace{\partial z_1 \dots z_1}_{m_1} \underbrace{\partial z_2 \dots z_2}_{m_2} \underbrace{\partial z_3 \dots z_3}_{m_3} \underbrace{\partial z_4 \dots z_4}_{m_4}.$$

For example

$$\langle r_1 r_2 p_2(p_2 - 1)(p_2 - 2) \rangle = \partial_{13444} F \Big|_{z=1},$$

because  $r_1$  is on the first position in the state  $q = (r_1, p_1, r_2, p_2)$ , and only one derivative with respect to  $z_1$  is required. The protein  $p_2$  is on the 4th position and it takes 3 derivatives to obtain  $p_2(p_2 - 1)(p_2 - 2)$ .

Instead of always showing that after a partial derivative we have to insert  $z = 1$  in the expression, we will use the following notation

$$\partial_m F |_{z=1} = F_m. \quad (\text{II.13})$$

For special examples like the one we work with, we can use suggestive notations for the indices  $z = (z_{r_1}, z_{p_1}, z_{r_2}, z_{p_2})$ . We list the first  $F_m$  variables in order as they appear in the Taylor expansion of the function  $F(z, t)$  about  $z = 1$ .

$$F_{r_1}, F_{r_2}, F_{p_1}, F_{p_2}, F_{r_1 r_1}, F_{r_1 p_1}, F_{r_1 r_2}, F_{r_1 p_2}, \dots, F_{p_2 p_2}, F_{r_1 r_1 r_1}, F_{r_1 r_1 r_2} \dots$$

These variables change in time as the generator  $G(t)$  drives the system. From these variables we can read the mean values of the molecules like  $\langle r_2 \rangle = F_{r_2}$  and also their standard deviation from the mean,  $\langle (r_2 - \langle r_2 \rangle)^2 \rangle = F_{r_2 r_2} + F_{r_2} - F_{r_2}^2$ . The time evolution of the variables  $F_m$  is a consequence of the Master Equation in  $F(z, t)$ :

$$\begin{aligned} \partial_t F(z, t) = & G(t)(z_{r_1} - 1)F(z, t) + \\ & \gamma_{r_1}(1 - z_{r_1})\partial_{z_{r_1}} F(z, t) + k_1(z_{p_1} - 1)z_{r_1}\partial_{z_{r_1}} F(z, t) + \gamma_{p_1}(1 - z_{p_1})\partial_{z_{p_1}} F(z, t) + \\ & h(z_{r_2} - 1)(z_{p_1}^2 \partial_{z_{p_1} z_{p_1}} F(z, t) + z_{p_1} \partial_{p_1} F(z, t)) + \\ & \gamma_{r_2}(1 - z_{r_2})\partial_{z_{r_2}} F(z, t) + k_2(z_{p_2} - 1)z_{r_2}\partial_{z_{r_2}} F(z, t) + \gamma_{p_2}(1 - z_{p_2})\partial_{z_{p_2}} F(z, t). \end{aligned} \quad (\text{II.14})$$

The right side of this equation is composed of three pieces. The first piece contains variables only from the System 1 (first 4 terms). Then comes a term proportional with the coupling constant  $h$  that show how the two systems are connected. The last three terms are specific to System 2. The coupling terms contain the second derivative with respect the protein 1, which is the input signal into the second system. Derivatives of order more than 1 are a sign of nonlinearity. Here the coupling transition probability  $T_{e_3}$  is a quadratic function in the protein number of System 1.

The time evolution equations of the  $F_m$  variables can be obtained from (II.14) by taking partial derivatives with respect to different combinations of the components of  $z$  and then inserting  $z = 1$ . Through this procedure, the partial differential equation for  $F(z, t)$  transforms into an infinite system of ordinary differential equations for the  $F_m$  variables (the tensor index  $m$  takes all the possible values). We present the first few:

$$\begin{aligned} \dot{F}_{r_1} &= G(t) - \gamma_{r_1} F_{r_1} \\ \dot{F}_{p_1} &= k_1 F_{r_1} - \gamma_{p_1} F_{p_1} \\ \dot{F}_{r_2} &= h(F_{p_1} + F_{p_1 p_1}) - \gamma_{r_2} F_{r_2} \\ \dot{F}_{p_2} &= k_2 F_{r_2} - \gamma_{p_2} F_{p_2} \\ \dot{F}_{r_1 p_2} &= G(t) F_{p_2} + k_2 F_{r_1 r_2} - (\gamma_{r_1} + \gamma_{p_2}) F_{r_1 p_2} \\ \dot{F}_{r_2 r_2} &= 2h(F_{p_1 r_2} + F_{p_1 p_1 r_2}) - 2\gamma_{r_2} F_{r_2 r_2}. \end{aligned}$$

If the system is linear, i.e. all the transition probabilities are linear in the state variables, then the infinite system can be closed to a finite one. Namely, if we collect all variables up to the modulus  $|\overline{m}| = \text{Max}(|\overline{m}| = m_1 + \dots + m_n)$ , than we create a system of equations that do not depend on a

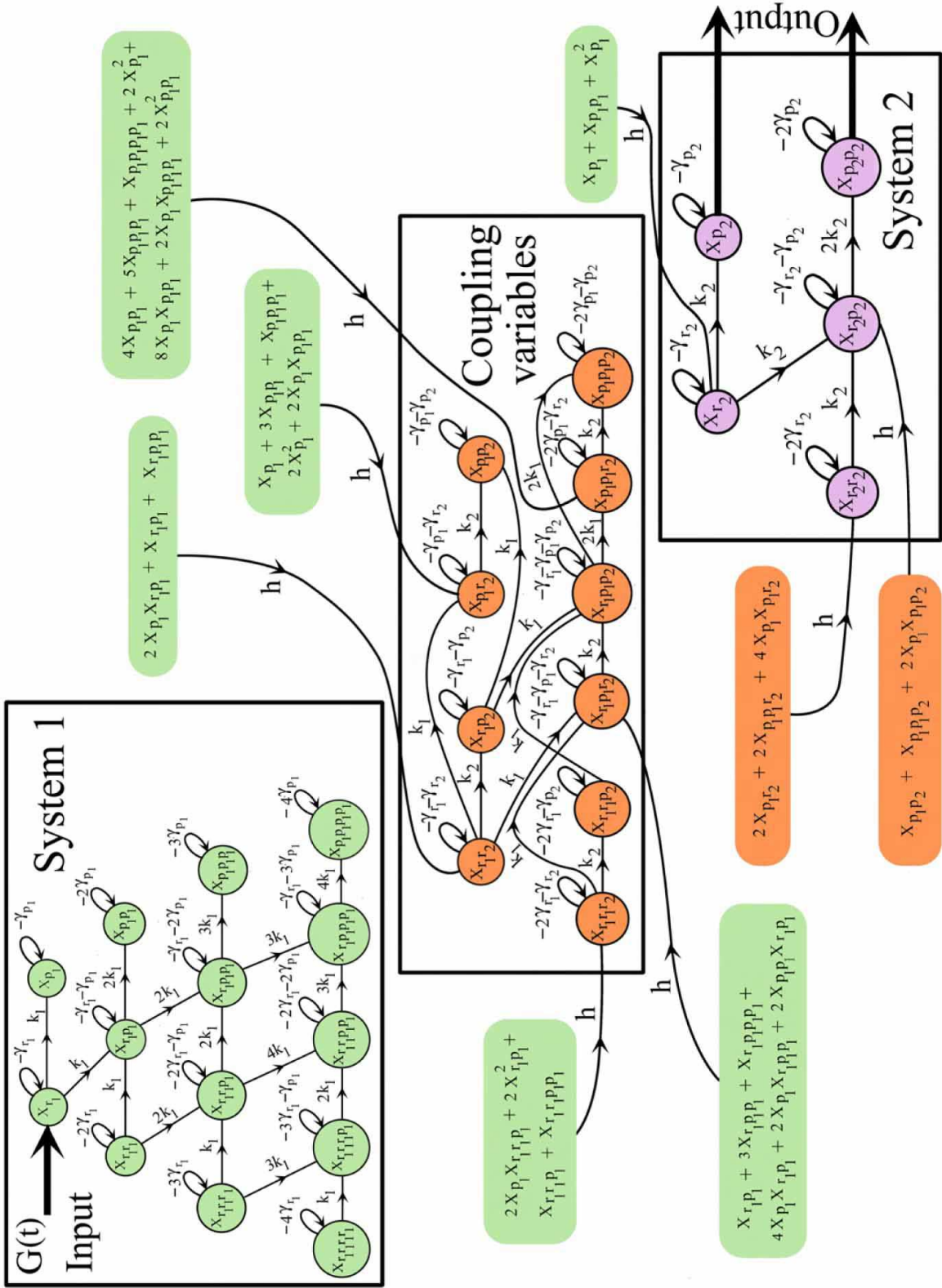


FIG. 3: Graph of the equations for the coupled systems.



$\bar{m}$  that has a modulus greater than  $Max$ . The system, being finite, is completely solvable [30]. For the nonlinear transition probabilities, the system is usually not finite. The variable  $F_m$  will depend on some other  $F_{m'}$  with  $|m'| > |m|$ .

Thus we need to cut the infinite system to obtain an ordinary system of equations: discard all  $F_m$ s with  $|m|$  greater than sum cutoff value. The problem that we run into is that the solution for variables  $F_m$  with small  $|m|$  depends on the cut even if the cut is taken at high values of  $|m|$ . Moreover, from a stable infinite system, by cutting we obtain an unstable system. The cause of this behavior is that as  $|m|$  increases, the values of  $F_m$  increases because it represents a mean of a high power polynomial in the state variables. Discarding such high values from the equations causes the aforementioned instability. However, a finite system can be obtained if instead of the variables  $F_m$  we change to a new set of variables that have small values that can be neglected for higher values of  $|m|$ . These variables represent for the factorial moments what cumulants represent for the classical moments [36]. The new function, call it  $X(z, t)$  is given by

$$F(z, t) = e^{X(z, t)}. \quad (\text{II.15})$$

The equation for the time evolution of  $X(z, t)$  is

$$\begin{aligned} \partial_t X(z, t) = & G(t)(z_{r_1} - 1) + \\ & \gamma_{r_1}(1 - z_{r_1})\partial_{z_{r_1}} X(z, t) + k_1(z_{p_1} - 1)z_{r_1}\partial_{z_{r_1}} X(z, t) + \gamma_{p_1}(1 - z_{p_1})\partial_{z_{p_1}} X(z, t) + \\ & h(z_{r_2} - 1) \left( z_{p_1}^2 \partial_{z_{p_1} z_{p_1}} X(z, t) + z_{p_1}^2 (\partial_{z_{p_1}} X(z, t))^2 + z_{p_1} \partial_{z_{p_1}} X(z, t) \right) + \\ & \gamma_{r_2}(1 - z_{r_2})\partial_{z_{r_2}} X(z, t) + k_2(z_{p_2} - 1)z_{r_2}\partial_{z_{r_2}} X(z, t) + \gamma_{p_2}(1 - z_{p_2})\partial_{z_{p_2}} X(z, t). \end{aligned}$$

We notice that the term proportional with  $h$  couples the two linear systems. Taking partial derivatives with respect to  $z$  and inserting  $z = 1$ , we obtain the variables  $X_m$ , indexed by the tensorial index  $m$ . The system of equations for these variables is represented as a graph in Fig. 3. Each node represents the time derivative of the variable written inside the node. A line entering the node corresponds to one term on the right side of the equation for that node; the term is the product of the variable written inside the start node and the coefficient above the line. For example, the equation for the variable  $X_{r_2 p_2}$  is

$$\dot{X}_{r_2 p_2} = k_2 X_{r_2} + k_2 X_{r_2 r_2} - (\gamma_{r_2} + \gamma_{p_2}) X_{r_2 p_2} + h(X_{p_1 p_2} + X_{p_1 p_1 p_2} + 2X_{p_1} X_{p_1 p_2}). \quad (\text{II.16})$$

The indices  $r_2 p_2$  of  $X_{r_2 p_2}$  belong to System 2 as well as three other terms that have indices from that same system. The term  $k_2 X_{r_2}$  is represented by the line starting on  $X_{r_2}$  and ending on the  $X_{r_2 p_2}$  node. The coupling coefficient  $h$  multiplies the polynomial combination  $X_{p_1 p_2} + X_{p_1 p_1 p_2} + 2X_{p_1} X_{p_1 p_2}$ . These polynomial combinations stem from the nonlinear coupling and their role is to connect System 1 with the System 2. If we are interested only in the mean value of the protein  $p_2$ , that is  $X_{p_2}$ , then we only need to solve the equations for the System 1, compute the coupling factor  $X_{p_1} + X_{p_1 p_1} + X_{p_1}$  and solve the equations for System 2. However, if we ask for the standard deviation of the number of protein molecules  $p_2$ , then we need  $X_{p_2 p_2}$  which requires solving for the coupling variables  $X_{r_1 r_2}, X_{r_1 p_2}, \dots, X_{p_1 p_1 p_2}$ , see Fig.3. When it comes to solving for the coupling variables, we find that variables up to fourth order in System 1 are necessary (like  $X_{r_1 r_1 r_1 r_1}$ ). In general, suppose we need to solve System 2 in order  $n$ , that is we need  $X_m$  with  $|m| = n$  and all components of the index  $m$  contain  $r_2$  or  $p_2$ . Then, we need an order  $n + 1$  in the coupling variables and  $n + 2$  in System 1. Another observation is that even if the coupling is nonlinear, the entire system of equations is finite. This property is a reminiscent of the fact that System 1 and 2 are linear. A linear system, whose equations are depicted in Fig. 3 in the upper left corner, has the

property that the order  $n$  depends only on orders that are smaller or equal to  $n$ . Thus, the equations for a linear system have a hierarchical structure, Fig 3, System 1. In [30] the equations for the first two orders for a linear system were solved. The second order variables like  $X_{r_1 r_1}, X_{p_1 p_1}$  were called non-Poisson components in [30]. This name came from the fact that the standard deviation can be expressed as  $\sigma_r^2 = X_r + X_{rr}$  and for a Poisson process  $\sigma_r^2 = X_r$ . We conclude this section by noting that two stochastic systems (System 1 and System 2) are not coupled by simply taking output variables from System 1 and input them into System 2. The stochastic coupling requires that the output of the System 1 should first pass through an intermediate system and then enter into the System 2.

## B. Molecular Diagrams

A graphical representation of gene regulatory networks is essential in order to capture information about gene interaction. A notational system should satisfy four important criteria [37]:

- (1) Expressiveness: the diagram should describe every possible relationship among molecules.
- (2) Semantically unambiguous: different symbols should be assigned to different semantics.
- (3) Extension capability: the notation system should be flexible, so that new symbols can be added in a consistent manner.
- (4) Mathematical translation: each diagram should be able to be converted into a mathematical formalism for use in quantitative computations.

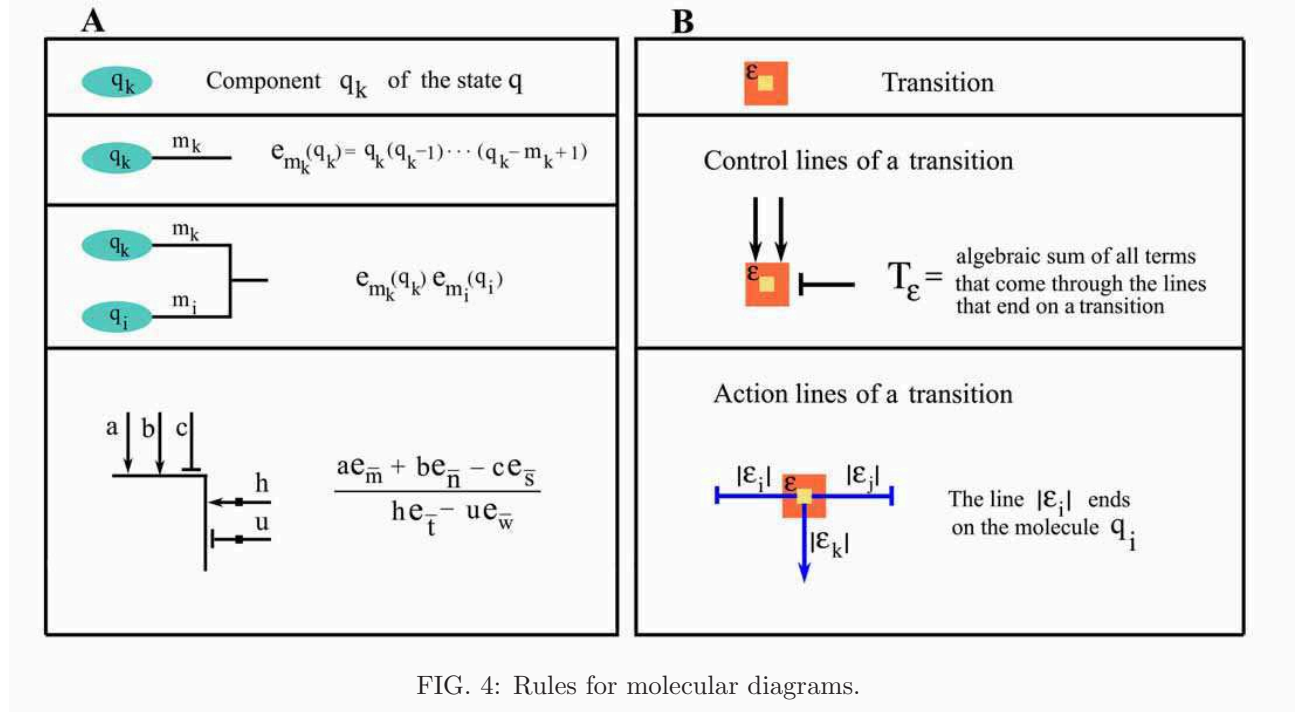


FIG. 4: Rules for molecular diagrams.

Based on the mathematical model for the stochastic genetic networks, we can assemble a set of rules to construct diagrams that obey the above criteria. The building blocks of the model are: the state  $q$ , the transitions  $\epsilon$  and the transition probabilities  $T_\epsilon$ . Each of these building blocks will be represented in a diagram, whose graphical notations are depicted in Fig. 4. The component  $q_k$  is represented by an oval, Fig. 4A, first row. If the molecules from a specific biological context are classified in families (antibodies, cytokines, etc.) then, instead of using an oval for each molecule,

a specific geometric shape can be associated with each family. For example, to distinguish between an mRNA and a protein, we used a quadrilateral symbol for mRNA and an oval for the protein. Each transition will be represented by a square, Fig. 4B first row. If necessary, the transitions can be grouped in phosphorylation, transport, transcription, etc. For each class of transition a different geometric symbol can be used. The transition probabilities are built upon decreasing factorials (II.8). A decreasing factorial  $\mathbf{e}_{m_k}(q_k)$  will be represented by a line starting from the component  $q_k$ , Fig. 4A second row. If the coefficient in front of a decreasing factorial is positive, the line will carry an arrow; otherwise the line will end in a bar. We will not write  $m_k$  on top of its corresponding line if  $m_k = 1$ . A product of two decreasing factorials is represented by joining the lines of each of the term in the product, Fig. 4A third row. Graphical representation of a rational function is depicted in Fig. 4A fourth row. The lines representing the terms from the denominator of the rational function are marked by a filled square. Two types of lines are associated with a transition  $\epsilon$ . One type ends on the border of the square representing the transition, Fig. 4B second row. These lines originate on different components  $q_k$  on which the transition probability  $T_\epsilon(q)$  depends. The components  $q_k$  control the transition probability  $T_\epsilon(q)$  so the lines that end on the boundary of the transition symbol are called *control lines*. Each transition will act on some molecules to change their number. This action is described by the components of the transition  $\epsilon$ . Each nonzero component of an  $\epsilon$  will be associated with a line that starts from the center of the transition symbol, Fig. 4B third row. These are called *action lines*. Each action line ends on a component  $q_k$  that is changed by the corresponding transition. If the component of a transition  $\epsilon$  is positive, the line is marked by an arrow and by a bar if the component is negative. In Fig. 4B third row,  $\epsilon_i < 0$ ,  $\epsilon_j < 0$  and  $\epsilon_k > 0$ . If  $|\epsilon_i| = 1$  we will not write it on its corresponding line. Finally, terms that correspond to lines that end on a transition  $\epsilon$  must be summed to form the transition probability, Fig. 4B second row. The molecular diagram for the system under study, Fig. 5, follows from Table 1 and the rules from Fig. 4.

The generator line has  $m = 0$  written on it, which corresponds to  $\mathbf{e}_{(0,0,0)} = 1$ , from Table 1. This line does not reach the center of the transition  $\epsilon_1$ , indicating that it is a control line. The transition is controlled by the generator and its transition probability is readable from the diagram:  $T_{\epsilon_1} = G(t)\mathbf{e}_{(0,0,0)} = G(t)$ . From the center of the transition  $\epsilon_1$  starts a line that points to the mRNA symbol  $r_1$ . This line, because it starts from the center, corresponds to the effect of the transition and tells that only one component of  $\epsilon_1$  is not zero,  $\epsilon_1 = (1, 0, 0)$ . The line has an arrow that indicates that this component is positive, so the transition will cause an increase of mRNA by one molecule. All other lines can be read in the same manner. From the protein  $p_1$  symbol there are two lines that control the transition  $\epsilon_3$ . These lines represent the nonlinear coupling  $T_{\epsilon_3} = hp_1^2 = hp_1 + hp_1(p_1 - 1)$  decomposed in the factorial bases. In Fig. 5, the line marked with the number 2 corresponds to the term  $hp_1(p_1 - 1)$  whereas the other line indicates the term  $hp_1$ . We will use molecular diagrams to present the interactions for each example that follows.

### C. Units of Measurement

The transition probabilities  $T_\epsilon(q, t)$  are measured in  $[\text{seconds}]^{-1}$  and thus the coefficient  $M_\epsilon^m(t)$  from  $T_\epsilon(q, t) = \sum_m M_\epsilon^m(t)\mathbf{e}_m(q)$  is measured in  $[\text{moles}]^{-|m|}[\text{seconds}]^{-1}$ . At present, the numerical values for the molecular constants  $M_\epsilon^m(t)$  that govern the mechanisms inside the cell can not be determined precisely through laboratory experiments. In what follows a numerical coefficients will be written without a unit of measurement, to show that it is not experimentally determined. We use numerical values to compare the analytical theory with Monte Carlo simulations and to show how the general formulas can be use in practical applications.

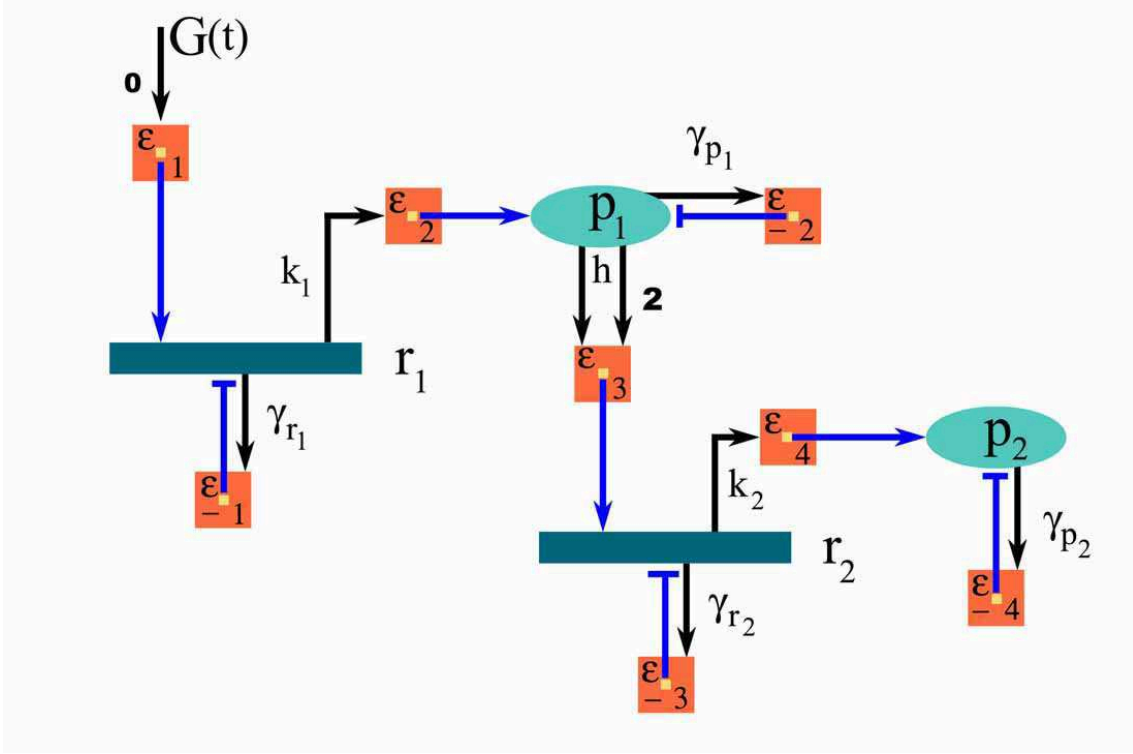


FIG. 5: Molecular diagram for two coupled systems

#### D. Hill Feedback Control

One of the basic elements of a gene regulatory network is a gene that controls its own transcription [38]. The protein acts on mRNA production through a term of the form

$$\frac{a}{b + p^2}. \quad (\text{II.17})$$

When the number of protein molecules increases, the rate of mRNA production will decrease, stabilizing the system's transcription and translation. This kind of feedback control is employed in the description of many biological systems. In [21] it is used to explain the appearance of multistability in the lactose utilization network of *Escherichia coli*. In [39] it is used to describe a stable oscillator constructed from three genes that repress themselves in a closed loop.

Our study focuses on the case where a signal generator accompanies the feedback. When the generator is turned off, the gene is driven slowly by the nonlinear feedback. This special case will be addressed in the following subparagraph. From a mathematical point of view, this system is interesting because the transition probability for repression is a rational function. The Table 2 and Fig.6 presents the structure of the system

The lines that do not start on any molecule represent the coefficients  $a_1$  and  $b_1$ . The coefficient  $b_1$ , being a term in the denominator of the feedback transition probability, has a small square superimposed upon it.

The Master Equation for the state probability is transformed by multiplying the whole equation (II.3) with  $b_1 + b_2 p + b_3 p(p - 1)$ .

TABLE 2: Hill Feedback Control

$\epsilon_1 = (1, 0)$	$\epsilon_{-1} = (-1, 0)$	$\epsilon_2 = (0, 1)$	$\epsilon_{-2} = (0, -1)$
$T_{\epsilon_1} = G(t) + \frac{a_1 + a_2 p}{b_1 + b_2 p + b_3 p(p-1)}$	$T_{\epsilon_{-1}} = \gamma_r r$	$T_{\epsilon_2} = K r$	$T_{\epsilon_{-2}} = \gamma_p p$

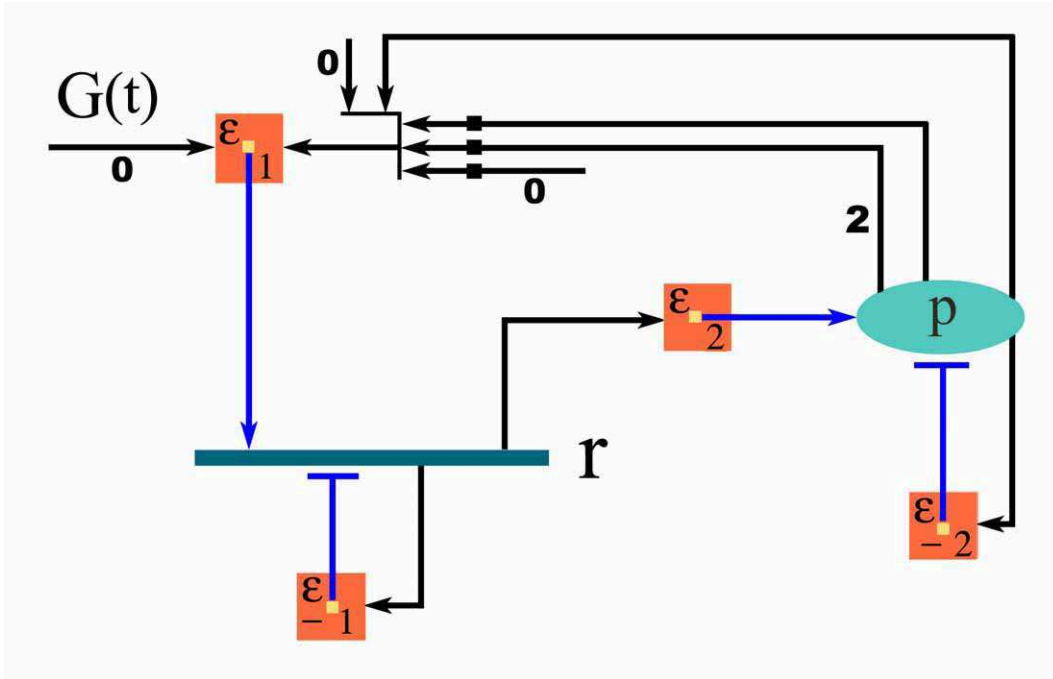


FIG. 6: Autoregulatory gene. The feedback has a Hill coefficient of 2.

$$\begin{aligned}
 (b_1 + b_2 p + b_3 p(p-1)) \frac{\partial}{\partial t} P(r, p, t) &= (a_1 + a_2 p) (P(r-1, p, t) - P(r, p, t)) + \\
 (b_1 + b_2 p + b_3 p(p-1)) [G(t) (P(r-1, p, t) - P(r, p, t)) &+ \gamma_r (r+1) P(r+1, p, t) - \gamma_r r P(r, p, t) + \\
 K r P(r, p-1, t) - K r P(r, p, t) + \gamma_p (p+1) P(r, p+1, t) - \gamma_p p P(r, p, t)] &.
 \end{aligned}$$

It is now possible to take the  $z$ -transform (II.5) and then change the variable from  $F(z, t)$  to  $X(z, t)$ , (II.15). The dynamical equation for  $X(z, t)$  contains both the effects of the nonlinear

feedback as well as the input signal generator  $G(t)$ :

$$\begin{aligned}
& b_1 \partial_t X + b_2 z_p (\partial_p \partial_t X + \partial_t X \partial_p X) + b_3 z_p^2 \left( \partial_{pp} \partial_t X + \partial_t X \partial_{pp} X + 2 \partial_p X \partial_t \partial_p X + (\partial_p X)^2 \partial_t X \right) = \\
& G(t) (z_r - 1) \left( b_1 + b_2 z_p \partial_p X + b_3 z_p^2 (\partial_{pp} X + (\partial_p X)^2) \right) + (z_r - 1) (a_1 + a_2 z_p \partial_p X) + \\
& \quad \gamma_r (1 - z_r) \left( b_1 \partial_r X + b_2 z_p (\partial_{rp} X + \partial_r X \partial_p X) + \right. \\
& \quad \left. b_3 z_p^2 (\partial_{rpp} X + \partial_{pp} X \partial_r X + 2 \partial_p X \partial_{rp} X + (\partial_p X)^2 \partial_r X) \right) + \\
& K z_r \left( b_1 (z_p - 1) \partial_r X + b_2 z_p \partial_r X + b_2 z_p (z_p - 1) (\partial_{rp} X + \partial_r X \partial_p X) + \right. \\
& \quad \left. 2 b_3 z_p^2 (\partial_{rp} X + (\partial_r X) \partial_p X) + \right. \\
& \quad \left. b_3 z_p^2 (z_p - 1) (\partial_{rpp} X + \partial_{pp} X \partial_r X + 2 \partial_p X \partial_{rp} X + (\partial_p X)^2 \partial_r X) \right) + \\
& \quad \gamma_p \left( b_1 (1 - z_p) \partial_p X - b_2 z_p \partial_p X + b_2 z_p (1 - z_p) (\partial_{pp} X + (\partial_p X)^2) - \right. \\
& \quad \left. 2 b_3 z_p^2 (\partial_{pp} X + (\partial_p X)^2) + \right. \\
& \quad \left. b_3 z_p^2 (1 - z_p) (\partial_{ppp} X + 3 \partial_{pp} X \partial_p X + (\partial_p X)^3) \right) .
\end{aligned}$$

The time dependent variables are the factorial cumulants and can be obtained from the Taylor expansion of  $X(z, t)$  about  $z = 1$ . Thus, we obtain an infinite number of equations; the first three of these are:

$$\begin{aligned}
& b_2 \dot{X}_p + b_3 \left( \dot{X}_{pp} + 2 X_p \dot{X}_p \right) = K \left( b_2 X_r + 2 b_3 (X_{rp} + X_r X_p) \right) \\
& - \gamma_p \left( b_2 X_p + 2 b_3 (X_{pp} + (X_p)^2) \right) , \tag{II.18}
\end{aligned}$$

$$\begin{aligned}
& b_1 \dot{X}_r + b_2 \left( X_p \dot{X}_r + \dot{X}_{rp} \right) + b_3 \left( 2 X_p \dot{X}_{rp} + X_{pp} \dot{X}_r + 2 X_{rp} \dot{X}_p + (X_p)^2 \dot{X}_r + \dot{X}_{rpp} \right) = \\
& G(t) \left( b_1 + b_2 X_p + b_3 (X_{pp} + (X_p)^2) \right) + a_1 + a_2 X_p \\
& - \gamma_r \left( b_1 X_r + b_2 (X_{rp} + X_r X_p) + b_3 (X_{rpp} + X_{pp} X_r + 2 X_p X_{rp} + (X_p)^2 X_r) \right) \\
& + K \left( b_2 (X_r + X_{rr}) + 2 b_3 (X_{rp} + X_r X_p + X_{rrp} + X_{rr} X_p + X_r X_{rp}) \right) \\
& - \gamma_p \left( b_2 X_{rp} + 2 b_3 (X_{rpp} + 2 X_p X_{rp}) \right) ,
\end{aligned}$$

$$\begin{aligned}
& b_1 \dot{X}_p + b_2 \dot{X}_p + b_2 \left( \dot{X}_{pp} + X_p \dot{X}_p \right) + 2 b_3 \left( \dot{X}_{pp} + 2 X_p \dot{X}_p \right) \\
& + b_3 \left( (X_p)^2 \dot{X}_p + 2 X_p \dot{X}_{pp} + \dot{X}_{ppp} + 3 X_{pp} \dot{X}_p \right) = \\
& K \left( b_1 X_r + b_2 (X_r + 2 X_{rp} + X_r X_p) + b_3 (4 X_{rp} + 4 X_r X_p + 4 X_p X_{rp} + 3 X_{pp} X_r + 3 X_{rpp} + (X_p)^2 X_r) \right) \\
& - \gamma_p \left( b_1 X_p + b_2 (X_p + 2 X_{pp} + (X_p)^2) + b_3 (4 X_{pp} + 4 (X_p)^2 + 3 X_{ppp} + 7 X_{pp} X_p + (X_p)^3) \right) . \tag{II.19}
\end{aligned}$$

If  $a_1 = 0$  and  $a_2 = 0$ , then the nonlinear feedback disappears and the system becomes linear. The equations then factorize into the simple equations discussed before for System 1, Fig. 3. When the

feedback is nonzero, that is  $a_1 \neq 0$  and  $a_2 \neq 0$ , the equations does not factorize. The left side of each equation in (II.18) is polynomial in the time derivative  $\dot{X}_m$  and  $X_m$ . This is characteristic for the rational transition probabilities, as will be proven in section 4. To assure that the transition probabilities are positive, we will work with a positive signal generator  $G(t) > 0$ . We will split the generator  $G(t)$  into a constant component  $G$  and a time variable component  $g(t)$

$$G(t) = G + g(t). \quad (\text{II.20})$$

For the constant component we take  $G = (G_{max} - G_{min})/2$  with  $G_{max}$  and  $G_{min}$  being the maximum and respectively the minimum value of  $G(t)$ . With this choice for  $G$  we have  $|g(t)| < G$ , so solutions to the equations (II.18) can be found by the method of expansion with respect to a small parameter. Namely, insert a parameter  $\eta$  in

$$G(t) = G + \eta g(t), \quad (\text{II.21})$$

and generate approximations,  $X_{m,k}$ , by collecting the like powers in  $\eta$  :

$$X_m(t) = X_{m,0} + \eta X_{m,1}(t) + \eta^2 X_{m,2}(t) + \dots ; \quad (\text{II.22})$$

then eliminate  $\eta$  by setting it to 1. The constant term  $G$  fixes a stationary level  $X_{m,0}$  that obeys a system of equations obtained from (II.18) by eliminating any time derivative and putting  $G$  instead of  $g(t)$ . The solution to the stationary case is interesting from a practical point of view and will explored it in the next paragraph; afterwards, we will return to study  $X_{m,1}(t)$ .

### 1. Designing the Shape of a Logic Pulse

In electrical engineering systems, properly connecting equipment along a signal path requires strict compliance with various standards. The logic 1's and 0's must be designed in such a way that they will be detected correctly after passing through chains of devices. A TTL device is guaranteed to interpret any input above 2 volts as a logic 1 or true and any input below 0.8 volts as a logic 0 or false; thus, there is a 1.2 volts protection against noise. Translating these ideas to a molecular device, we want to use the autoregulatory system to generate a logic pulse in protein numbers. Then let  $G_1$  be the input signal for a protein level that represents a logic 0 and  $G_2$  for a logic 1.

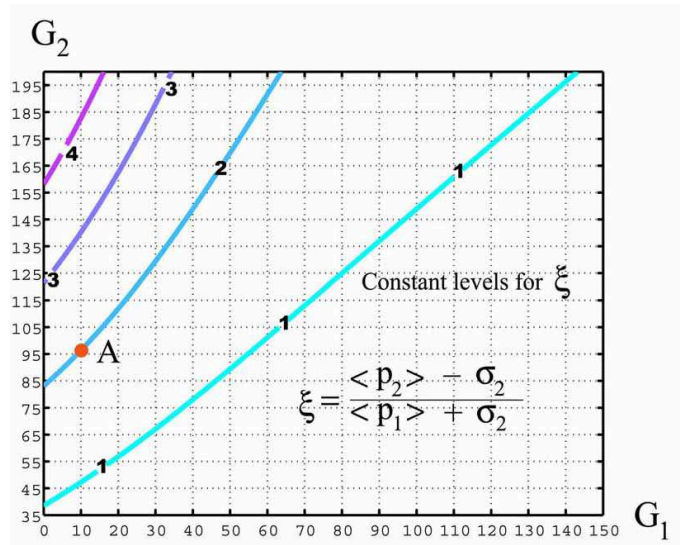


FIG. 7: Constant Levels for  $\xi$ .

Because the system is intrinsically stochastic the logic levels refer to the mean values of the protein,  $\langle p_1 \rangle$  and  $\langle p_2 \rangle$  respectively. The protein values will fluctuate around these mean values. A measure of this fluctuation is the standard deviation of the protein numbers  $\sigma_1 = \sqrt{\langle (p_1 - \langle p_1 \rangle)^2 \rangle}$  and similar for  $\sigma_2$ . To separate the logical levels we will ask that the following ratio:

$$\xi = \frac{\langle p_2 \rangle - \sigma_2}{\langle p_1 \rangle + \sigma_1} \quad (\text{II.23})$$

be high enough. The constant contour plot of the ratio  $\xi$  is presented in Fig. 7 for the following set of numerical parameters

$$\{\gamma_r = 2, \gamma_p = 1, K = 0.5, a_1 = 1, a_2 = 0, b_1 = 0.01, b_2 = 0.001, b_3 = 0.001\} . \quad (\text{II.24})$$

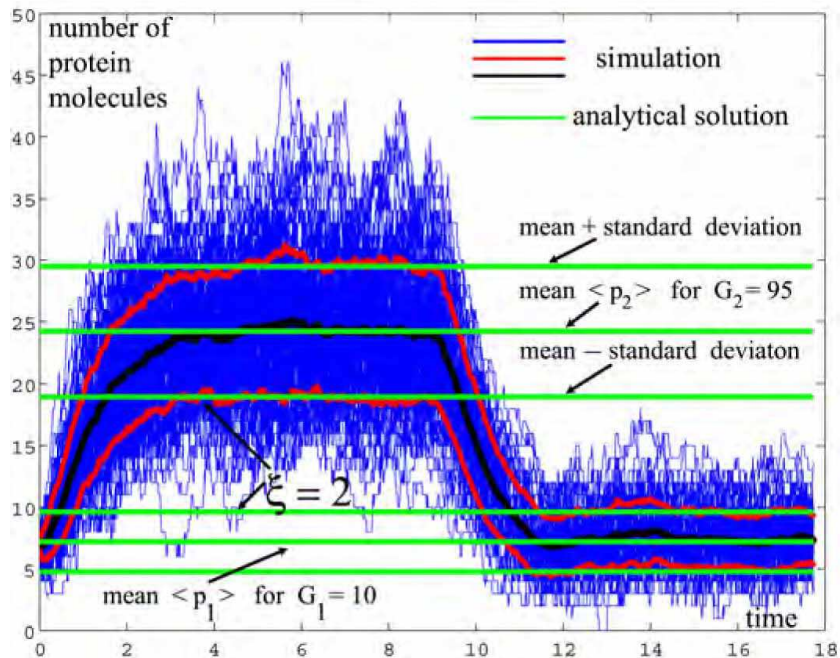


FIG. 8: Pulse design.

To design a shape for a pulse we first fix  $G_1$  for the logic 0 and then choose a value for the ratio  $\xi$ . From Fig. 7 we read the input  $G_2$  for the logic 1. For example, if  $G_1 = 10$  and  $\xi = 2$  we obtain  $G_2 = 95$ , which is the point A on the graph. The pulse for these values is shown in Fig. 8. This figure also shows that the analytical values are confirmed by a Monte Carlo simulation using the direct Gillespie algorithm, see Materials and Methods. The simulated means and standard deviations are based on 500 independent stochastic processes. The pulse is separated from the baseline level by a factor of  $\xi = 2$  and only a few of the simulations drop down in the region  $\langle p_1 \rangle \pm \sigma_1$ . The comparison of the analytic formulas with the Monte Carlo results proves the power of the method outlined, especially that the variables  $X_m$  are well suited for numerical computations. The next paragraph, and other examples that follow, will show the effectiveness of the factorial cumulants.

## 2. The Autoregulatory Gene Driven Only by its Protein Level

If  $G = 0$ , the generator is closed, leaving only the feedback to sustain the mRNA production. An equilibrium between mRNA and the protein level will take place. Using the traditional method



of mass action (chemical equilibrium), we can compute this equilibrium by equating the production rates with the degradation rates:

$$\frac{a_1 + a_2 p}{b_1 + b_2 p + b_3 p(p-1)} = \gamma_r r, \quad (\text{II.25})$$

$$kr = \gamma_p p. \quad (\text{II.26})$$

The mass action procedure assumes that the stochastic process is Poisson, so the size of the standard deviation from the mean equals the square root of the mean. We found that the mass action procedure does not explain the data obtained from Monte Carlo simulations, Fig. 9 and Table 3. However, we match the simulations by solving the first  $N$  equations of the infinite system of equations (II.18). As  $N$  increases, the solutions more closely approach the simulated data; see Fig. 9 where  $N = 7$  and 15.

**TABLE 3: Analytical Solutions Explain Monte Carlo Simulations**

	Monte Carlo	15 equations	7 equations	mass action
mean	12.38	12.37	12.16	11.54
mean + standard deviation	17.55	17.50	16.76	14.94

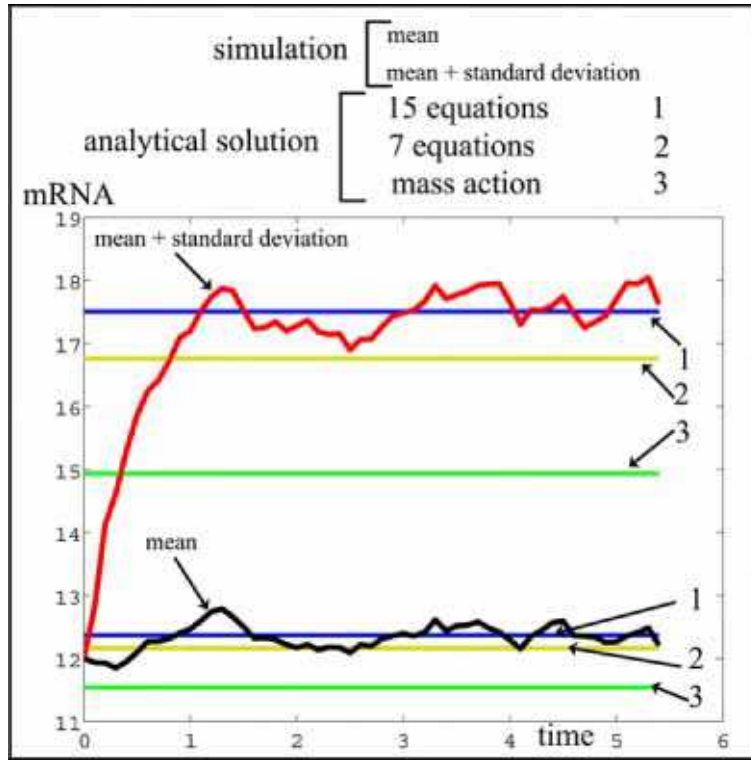


FIG. 9: Analytical solution explaining the simulated data.

As we take more equations we obtain better results, so the variables  $X_m$  (factorial cumulants) are suited for numerical and analytical approximations. The conclusion is that the mean values depend on cumulants of higher orders and thus equations that mix the means with cumulants of higher orders must be solved simultaneously.

### 3. Response of the Nonlinear Autoregulatory Gene to a Time Variable Input Signal Generator

The generator is now time dependent (II.21)

$$G(t) = G + g(t)$$

The solution in the first order, (II.22), is  $X_m(t) = X_{m,0} + X_{m,1}(t)$ . At this point we can move from tensor notations to a matrix notation to present the solutions in the usual form for input-output relations from control theory. We construct thus column vectors  $X_{(0)}$  and  $X_{(1)}$  using the lexicographic order for the tensor index  $m$ . For example

$$X_{(1)} = [X_{r,1}, X_{p,1}, X_{rr,1}, X_{rp,1}, X_{pp,1}, \dots]^t. \quad (\text{II.27})$$

which is written in a transposed form to save space.

Using (II.21) and equating the terms which contain  $\eta$  from both sides of (II.18) we obtain a linear time evolution equation for  $X_{(1)}$

$$E\dot{X}_{(1)} = A X_{(1)} + B g(t), \quad (\text{II.28})$$

where  $E$  and  $A$  are infinite square matrices and  $B$  is an infinite column vector. The entries of these matrices depend on the parameters of the system as well as the stationary solution vector  $X_{(0)}$ . From these infinite systems of equations we construct a finite system with a dimension depending on how many orders for the factorial cumulants  $X_m$  we want to keep (that is what is the maximum value for  $|m|$  we need). To obtain a nonsingular matrix  $E$  the first equation in (II.18) must be omitted. This equation is a consequence of the transition probabilities being a rational function. If the transition probabilities were only polynomials in the state variables, then this first equation will become a trivial  $0 = 0$ . A  $2 \times 2$  finite system will have the following matrices:

$$E = \begin{bmatrix} b_1 + b_2 X_{p,0} + b_3 X_{pp,0} + b_3 X_{p,0}^2 & 2 b_3 X_{rr,0} \\ 0 & b_1 + b_2 + b_2 X_{p,0} + 4 b_3 X_{p,0} + 3 b_3 X_{pp,0} + b_3 X_{p,0}^2 \end{bmatrix}$$

$$A_{1,1} = -\gamma_r (b_1 + b_2 X_{p,0} + b_3 (X_{pp,0} + X_{p,0}^2)) + k (b_2 + 2 b_3 X_{p,0}) + 2 k b_3 X_{rp,0}$$

$$A_{1,2} = G (b_2 + 2 b_3 X_{p,0}) + a_2 - \gamma_r (b_2 X_{r,0} + b_3 (2 X_{rp,0} + 2 X_{r,0} X_{p,0})) \\ + 2 k b_3 X_{r,0} + 2 k b_3 X_{rr,0} - 4 \gamma_p b_3 X_{rp,0}$$

$$A_{2,1} = k (b_1 + b_2 + b_2 X_{p,0} + 4 b_3 X_{p,0} + 2 b_3 X_{pp,0} + b_3 (X_{pp,0} + X_{p,0}^2))$$

$$A_{2,2} = k (b_2 X_{r,0} + 4 b_3 X_{r,0} + 2 b_3 X_{rp,0} + b_3 (2 X_{rp,0} + 2 X_{r,0} X_{p,0})) - \\ \gamma_p (b_1 + b_2 + 2 b_2 X_{p,0} + 8 b_3 X_{p,0} + 4 b_3 X_{pp,0} + b_3 (3 X_{pp,0} + 3 X_{p,0}^2))$$

$$B = \begin{bmatrix} b_1 + b_2 X_{p,0} + b_3 (X_{pp,0} + X_{p,0}^2) \\ 0 \end{bmatrix}.$$

However, finite systems of larger dimensions are needed to obtain accurate solutions for the mean and standard deviations of the molecule numbers. Large systems of equations are easily generated

with symbolic software like Maple or Mathematica; however, these equations are too large to be displayed within the article. However, using numerical values (II.24) and  $G = 30$  we can go further and display the final results. The stationary point solution up to the second order

$$X_{r,0} = 20.251, X_{p,0} = 10.125, X_{rr,0} = 0.909, X_{rp,0} = -0.935, X_{pp,0} = -0.468 \quad (\text{II.29})$$

shows that the mean value for mRNA is about 20 molecules and the protein number is about 10. The factorial cumulants of higher order have absolute values smaller than the corresponding factorial moments. For example  $F_{rr,0}$  would be of order  $20(20 - 1) = 380$  whereas  $X_{rr,0}$  is about 1.

In the spirit of control theory, the solution to (II.28) can be written as an input-output relation using the Laplace transform of the  $X_{m,1}$  variables:

$$\begin{aligned} X_{p,1}(s) &= \frac{0.50 (s + 5.93) (s + 2.50) (s^2 + 5.94 s + 11.9)}{(s^2 + 3.0 s + 2.62) (s^2 + 4.14 s + 6.87) (s^2 + 10.2 s + 29.0)} g(s) \\ X_{pp,1}(s) &= \frac{0.0075 (s + 65.9) (s + 2.04) (s^2 + 10.2 s + 29.8)}{(s^2 + 3.0 s + 2.62) (s^2 + 4.14 s + 6.87) (s^2 + 10.2 s + 29.0)} g(s) \end{aligned} \quad (\text{II.30})$$

Thus the mean and the fluctuation of the protein number can be directly related with the input signal  $g(s)$  which is the Laplace transform of  $g(t)$ .

### E. Michaelis-Menten Amplifier

Catalytic enzymatic processes, like phosphorylation, are fundamental for biological processes. The process requires a substrate S reacting with an enzyme E to form a complex C which in turn is converted into a product P and the enzyme E, Fig. 10. In a test tube, the reaction proceeds in one direction, that is  $k_{-1} = 0$  and  $k_{-2} = 0$  which is a special case of Fig. 10. However, it is possible that in a cell a more general scheme where  $k_{-1} \neq 0$  and  $k_{-2} \neq 0$  can take place [40]; thus we study the case in Fig. 10. The substrate S is usually supplied in large quantities compared with the enzyme E, and the goal of the process is to transform the substrate S into the product P. We choose an input oscillatory signal generator to act on the enzyme E. Then, we follow the signal through the complex C to the output product P. It is possible to drive large oscillations in the product P using small oscillations in the enzyme E. In this case the catalytic process behaves like a molecular amplifier. This situation is analogous with how a transistor amplifies the input signal on its base. A constant voltage source is necessary to supply the energy for the electrical amplification. Here the role of the source is played by the substrate S, the signal in the transistor's base by the enzyme E and the output signal from the transistor's collector by the product P. The state is  $q = (E, S, C, P)$  and the transition probabilities are polynomials in the state variables, Table 4. The molecular diagram, Fig. 11, depicts all possible transitions in the system and which variables control these transitions.

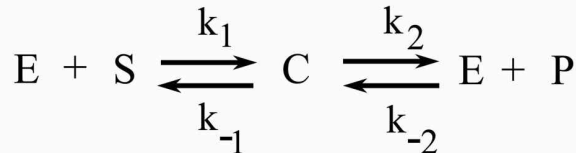


FIG. 10: Catalytic reaction.

TABLE 4: Michaelis-Menten Process

$\epsilon_1 = (1, 0, 0, 0)$	$T_1 = G(t)$	$\epsilon_3 = (-1, -1, 1, 0)$	$T_3 = k_1 E \cdot S$
$\epsilon_{-1} = (-1, 0, 0, 0)$	$T_{-1} = \gamma_E E$	$\epsilon_{-3} = (1, 1, -1, 0)$	$T_{-3} = k_{-1} C$
$\epsilon_2 = (0, 1, 0, 0)$	$T_2 = K_S$	$\epsilon_4 = (1, 0, -1, 1)$	$T_4 = k_2 C$
$\epsilon_{-2} = (0, -1, 0, 0)$	$T_{-2} = \gamma_S S$	$\epsilon_{-4} = (-1, 0, 1, -1)$	$T_{-4} = k_{-2} E \cdot P$
$\epsilon_{-5} = (0, 0, 0, -1)$	$T_{-5} = \gamma_P P$		

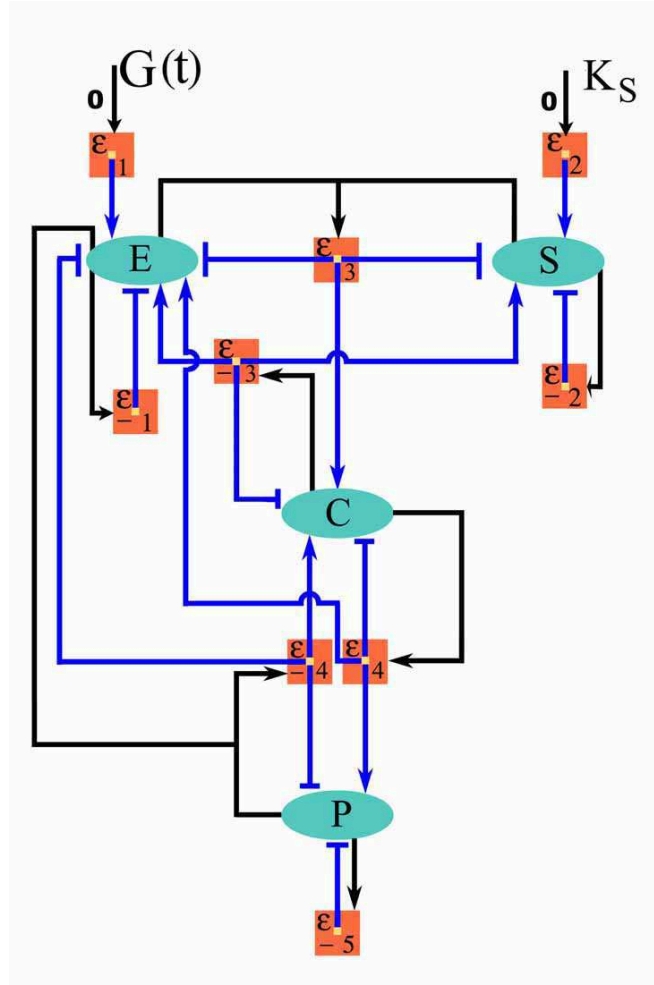


FIG. 11: Molecular diagram for Michaelis-Menten process.

The transition probabilities will generate a stochastic process described by the time evolution of its factorial cumulants:

$$\begin{aligned} \partial_t X = & k_1(z_C - z_E z_S) (\partial_{z_E z_S} X + \partial_{z_E} X \partial_{z_S} X) + k_{-1}(z_E z_S - z_C) \partial_{z_C} X + k_2(z_E z_P - z_C) \partial_{z_C} X \\ & + G(t)(z_E - 1) + \eta_E(1 - z_E) \partial_{z_E} X + \eta_S(1 - z_S) \partial_{z_S} X + \eta_P(1 - z_P) \partial_{z_P} X \\ & + k_{-2}(z_C - z_E z_P) (\partial_{z_E z_P} X + \partial_{z_E} X \partial_{z_P} X) + K_S(z_S - 1). \end{aligned}$$

The term  $G(t)(z_E - 1)$  represents the time variable input generator which acts on the enzyme  $E$ , whereas  $K_S(z_S - 1)$  comes from the constant production of the source  $S$ . An advantage of the variable  $X(z, t)$  is that the generator terms do not contain the variable  $X(z, t)$ . This will translate into equations with constant coefficients for the  $X_m$  variables:

$$\begin{aligned}
\dot{X}_E &= -k_1(X_{ES} + X_EX_S) + k_{-1}X_C + k_2X_C + G(t) - \gamma_EX_E \\
&\quad - k_{-2}(X_{EP} + X_EX_P) , \\
\dot{X}_S &= -k_1(X_{ES} + X_EX_S) + k_{-1}X_C - \gamma_SX_S + K_S , \\
\dot{X}_C &= k_1(X_{ES} + X_EX_S) - k_{-1}X_C - k_2X_C + k_{-2}(X_{EP} + X_EX_P) , \\
\dot{X}_P &= k_2X_C - \gamma_PX_P - k_{-2}(X_{EP} + X_EX_P) , \\
\dot{X}_{EE} &= -2k_1(X_{EE}X_S + X_EX_{ES}) + 2k_{-1}X_{EC} + 2k_2X_{EC} - 2\gamma_EX_{EE} \\
&\quad - 2k_{-2}(X_{EE}X_P + X_EX_{EP}) , \\
\dot{X}_{ES} &= -k_1(X_{ES} + X_EX_S) - k_1(X_{ES}X_S + X_EX_{SS}) - k_1(X_{EE}X_S + X_EX_{ES}) \\
&\quad + k_{-1}X_C + K_{-1}X_{SC} + k_{-1}X_{EC} \\
&\quad + k_2X_{SC} - \gamma_EX_{ES} - \gamma_SX_{ES} - k_{-2}(X_{ES}X_P + X_EX_{SP}) , \\
\dot{X}_{EC} &= -k_1(X_{EC}X_S + X_EX_{SC}) + k_1(X_{EE}X_S + X_EX_{ES}) \\
&\quad + k_{-1}X_{CC} - k_{-1}X_{EC} + k_2X_{CC} - k_2X_{EC} \\
&\quad - \gamma_EX_{EC} - k_{-2}(X_{EC}X_P + X_EX_{CP}) + k_{-2}(X_{EE}X_P + X_EX_{EP}) , \\
\dot{X}_{EP} &= -k_1(X_{EP}X_S + X_EX_{SP}) + k_{-1}X_{CP} + k_2X_C + k_2X_{CP} + k_2X_{EC} - \gamma_EX_{EP} \\
&\quad - \gamma_PX_{EP} - k_{-2}(X_{EP} + X_EX_P) - k_{-2}(X_{EP}X_P + X_EX_{PP}) \\
&\quad - k_{-2}(X_{EE}X_P + X_EX_{EP}) , \\
\dot{X}_{SS} &= -2k_1(X_{ES}X_S + X_EX_{SS}) + 2k_{-1}X_{SC} - 2\gamma_SX_{SS} , \\
\dot{X}_{SC} &= -K_1(X_{EC}X_S + X_EX_{SC}) + k_1(X_{ES}X_S + X_EX_{SS}) + k_{-1}X_{CC} \\
&\quad - k_{-1}X_{SC} - k_2X_{SC} - \gamma_SX_{SC} + k_{-2}(X_{ES}X_P + X_EX_{SP}) , \\
\dot{X}_{SP} &= -k_1(X_{EP}X_S + X_EX_{SP}) + k_{-1}X_{CP} + k_2X_{SC} - \gamma_SX_{SP} - \gamma_PX_{SP} \\
&\quad - k_{-2}(X_{ES}X_P + X_EX_{SP}) , \\
\dot{X}_{CC} &= 2k_1(X_{EC}X_S + X_EX_{SC}) - 2k_{-1}X_{CC} \\
&\quad - 2k_2X_{CC} + 2k_{-2}(X_{EC}X_P + X_EX_{CP}) , \\
\dot{X}_{CP} &= k_1(X_{EP}X_S + X_EX_{SP}) - k_{-1}X_{CP} - k_2X_{CP} + k_2X_{CC} \\
&\quad - \gamma_PX_{CP} + k_{-2}(X_{EP}X_P + X_EX_{PP}) - k_{-2}(X_{EC}X_P + X_EX_{CP}) , \\
\dot{X}_{PP} &= 2k_2X_{CP} - 2\gamma_PX_{PP} - 2k_{-2}(X_{EP}X_P + X_EX_{PP}) .
\end{aligned} \tag{II.31}$$

The generator  $G(t) = G + g(t)$  will determine a stationary state by  $G$  and a time variation by  $g(t)$ . For an oscillatory input of the form

$$G(t) = G + G \cos(\omega t) \tag{II.32}$$

and for the following numerical coefficients

$$\{\gamma_P = 1, K_{-2} = 1, K_1 = 0.1, K_2 = 6, K_S = 50, G = 300, \gamma_S = 0.003, K_{-1} = 0.1, \gamma_E = 50\} ,$$

the stationary state is

$$\{X_{E,0} = 6.00, X_{S,0} = 92.71, X_{C,0} = 58.14, X_{P,0} = 49.72, X_{EE,0} = -0.04, X_{ES,0} = -.88, X_{EC,0} = 0.04, X_{EP,0} = 0.76, X_{SS,0} = 12.28, X_{SC,0} = -7.82, X_{SP,0} = -1.23, X_{CS,0} = 3.10, X_{CP,0} = 3.60, X_{PP,0} = -2.33\}.$$

The stationary state was solved up to the second order cumulants using the equations (II.31). In the first order, the time variation of the  $X_m$  variables is  $X_m(t) = X_{m,0} + X_{m,1}(t)$ , (II.22). Each variable  $X_{m,1}(t)$  will contain an oscillatory component  $A_m(\omega)e^{i\omega t}$ . As a function of  $\omega$ , and for the parameters considered above, the ratio between the amplitude of the protein oscillations and the amplitude of the enzyme oscillations is presented in Fig. 12. The maximum of this ratio is 3.71 at  $\omega = 3$ .

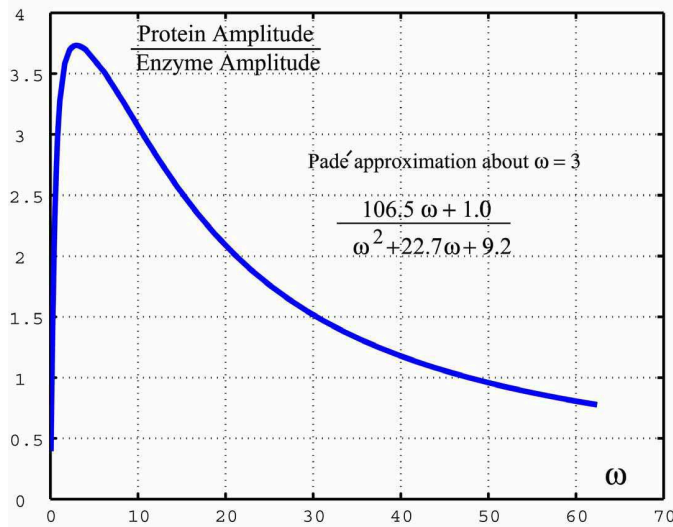


FIG. 12: Protein amplification,  $\frac{|A_P(\omega)|}{|A_E(\omega)|}$ .

A Padé approximation about  $\omega = 3$  for the amplitudes' ratio is

$$\frac{|A_P(\omega)|}{|A_E(\omega)|} \approx \frac{106.5\omega + 1.0}{\omega^2 + 22.7\omega + 9.2}. \quad (\text{II.33})$$

The frequency  $\omega$  is measured in  $[time]^{-1}$ , see section C. Thus, the enzyme oscillations are amplified as they pass to the product P, Fig. 12. So far, we analyzed stationary solutions and stationary periodic regimes. Another question to address is how the system behaves in a transitory regime. We did 500 Monte Carlo simulations for the system that starts at the time  $t = 0$  from the zero initial conditions (all molecule numbers are zero). As the energy is pumped into the system by the signal generator  $G(t) = G + G \cos(\omega t)$ , the molecule numbers will grow towards a stable periodic state. The transitory process is an oscillatory variation superimposed on a growing exponential trend, Fig. 13. The numerical solution of the equations (II.31), show that the simulated data are explained by the dynamical equations. The error measured by the  $L_2$  norm of the difference between the simulated data and the computed data is 1% of the norm of the simulated data. Thus we can work with numerical solutions to (II.31) instead of using Monte Carlo simulations. Moreover, on (II.31) we can apply a different analytical approximation (i.e. harmonic balance, expansion in a small parameter) which can capture the behavior of the system as a function of its parameters. We observe, Fig. 13, that the product oscillates in antiphase with respect to the enzyme, a phenomenon also present also in a basic transistor amplifier.

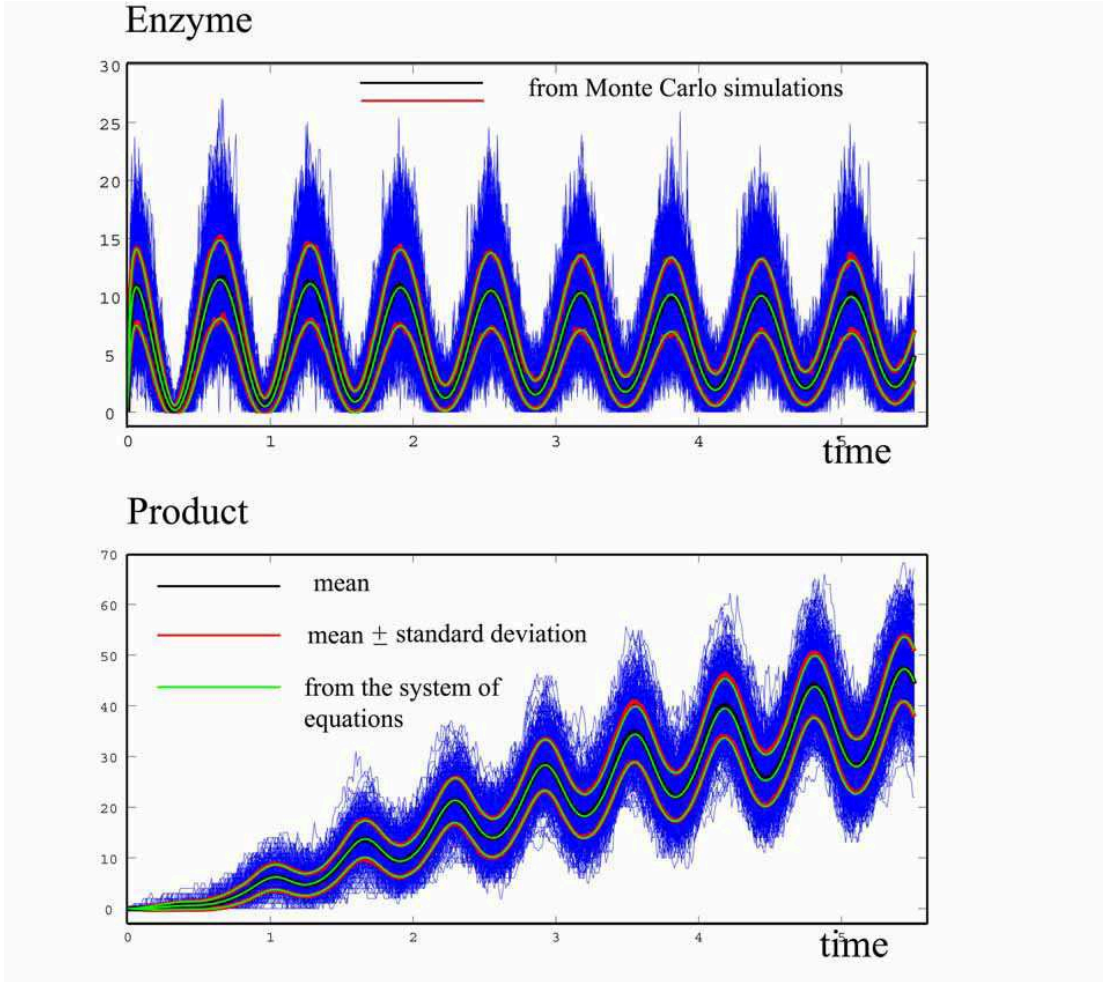


FIG. 13: Transitory regime: Numerical solutions of the equations (II.31) agree with Monte Carlo simulations.

### F. E2F1 Regulatory Element

The systems studied in the preceding paragraphs were excited by one signal generator. There are many cases in living organisms where a gene is regulated by more than one signal. In what follows we will study a regulatory element inspired by the E2F1, a member of the E2F family of transcription factors [41]. In addition to its established proliferative effect, E2F1 has also been implicated in the induction of apoptosis through p53-dependent and p53-independent pathways [42]. The components of the E2F1 system were described in [43]. The mRNA level, Fig.14, is regulated by 3 transcription factors E2F1, pRb and DP1. The regulation is done by the dimer E2F1:DP1 which, for short, is denoted by the letter  $a$ . This dimer binds to the DNA and its effect is to increase the rate of transcription. The second control of transcription is from the complex  $a:pRB$ , that binds to the DNA and repress the transcription. The state of the system is thus an 8 component vector  $q = (E2F1, DP1, pRB, a, b, c, d, mRNA)$ . This example shows that a state is not just a list of different species of molecules. The same dimer E2F1:DP1 is present in the state vector as a component  $a$  unbound to DNA and a state component  $c$  when the dimer is bound to the DNA. These are 2 different situations of the same molecular species and we treat them as different components of the state of the system. In the diagram of Fig. 14, we use an oval glued to a rectangle

**TABLE 5: E2F1 Regulatory Element**

$\epsilon_1 = (1, 0, 0, 0, 0, 0, 0, 0)$	$T_{\epsilon_1} = G_1(t)$	$\epsilon_{-1} = (-1, 0, 0, 0, 0, 0, 0, 0)$	$T_{\epsilon_{-1}} = k_{-1} E2F1$
$\epsilon_2 = (0, 1, 0, 0, 0, 0, 0, 0)$	$T_{\epsilon_2} = G_2(t)$	$\epsilon_{-2} = (0, -1, 0, 0, 0, 0, 0, 0)$	$T_{\epsilon_{-2}} = k_{-2} DP1$
$\epsilon_3 = (0, 0, 1, 0, 0, 0, 0, 0)$	$T_{\epsilon_3} = G_3(t)$	$\epsilon_{-3} = (0, 0, -1, 0, 0, 0, 0, 0)$	$T_{\epsilon_{-3}} = k_{-3} pRb$
$\epsilon_4 = (-1, -1, 0, 1, 0, 0, 0, 0)$	$T_{\epsilon_4} = k_4 E2F1 \cdot DP1$	$\epsilon_{-4} = ((1, 1, 0, -1, 0, 0, 0, 0)$	$T_{\epsilon_{-4}} = k_{-4} a$
$\epsilon_5 = (0, 0, 0, -1, 0, 1, 0, 0)$	$T_{\epsilon_5} = k_5 a (n_1 - n_2 c - n_3 d)$	$\epsilon_{-5} = (0, 0, 0, 1, 0, -1, 0, 0)$	$T_{\epsilon_{-5}} = k_{-5} c$
$\epsilon_6 = (0, 0, -1, -1, 1, 0, 0, 0)$	$T_{\epsilon_6} = k_6 a \cdot pRb$	$\epsilon_{-6} = (0, 0, 1, 1, -1, 0, 0, 0)$	$T_{\epsilon_{-6}} = k_{-6} b$
$\epsilon_7 = (0, 0, 0, 0, -1, 0, 1, 0)$	$T_{\epsilon_7} = k_7 b (m_1 - m_2 c - m_3 d)$	$\epsilon_{-7} = (0, 0, 0, 0, 1, 0, -1, 0)$	$T_{\epsilon_{-7}} = k_{-7} d$
$\epsilon_8 = (0, 0, 0, 0, 0, 0, 0, 1)$	$T_{\epsilon_8} = k_8 c (l_1 - l_2 d)$	$\epsilon_{-8} = (0, 0, 0, 0, 0, 0, 0, -1)$	$T_{\epsilon_{-8}} = k_{-8} r$

to graphically depict the DNA-bound form of a transcription factor. The transition probability that controls the mRNA production is  $T_{\epsilon_8} = k_8(l_1 - l_2d)$ , Table 5. The transition  $\epsilon_8$  is upregulated by  $c$  so  $T_{\epsilon_8}$  is proportional to  $c$ . The repression by  $d$  is described by the term  $l_1 - l_2d$  chosen to obey two criteria: (1) it decreases as  $d$  increases, and (2) is positive so the transition probability will be a positive number. A specified set of parameters together with a solution to the equation of motions are realistic if the transition probabilities stay positive or zero for any instant of time. One control line starting from  $c$  ends with an arrow on the transition  $\epsilon_8$  which signifies that  $c$  upregulates the transcription. This control line corresponds to the term  $k_8 l_1 c$  from  $T_{\epsilon_8}$ . Another control line starts from  $c$  and  $d$  and ends in a short bar, thus repressing the mRNA transcription. This line represents the term  $-k_8 l_2 c d$  from  $T_{\epsilon_8}$ . Variations in the number of  $c$  and  $d$  molecules will depend on variations in E2F1, DP1 and pRB. Thus we will insert 3 signal generators  $G_1(t)$ ,  $G_2(t)$  and  $G_3(t)$  to modulate the levels of E2F1, DP1 and pRB respectively. The transitions  $\epsilon_i$ , with  $i = 1, 2, 3$ , represent these input generators. The degradation transitions  $\epsilon_{-i}$ ,  $i = 1, 2, 3$ , are taken to be proportional with the number of molecules being degraded. The formation of the dimer  $a$  is described by  $\epsilon_4$  which is controlled by a nonlinear transition probability (the product of E2F1 with DP1). The transition  $\epsilon_5$  represents the binding of the dimer  $a$  to DNA. That is the creation of one  $c$  from one  $a$ , as is readable from the components of the transition  $\epsilon_5$ . The transition probability for this binding event is proportional to the number of  $a$  dimers and with the free space available on the DNA. This free space available for DNA binding should be of the form  $n - c - d$  where  $n$  is the maximum number of proteins that can bind to DNA to regulate the transcription. We subtract from  $n$  the space already occupied which is  $c + d$ . In order to cover the situation when the binding properties of  $c$  and  $d$  are different we use  $T_{\epsilon_5} = k_5 a (n_1 - n_2 c - n_3 d)$ , with  $n_1, n_2$  and  $n_3$  some constant coefficients. Then, the transition  $\epsilon_6$  is like  $\epsilon_4$  and  $\epsilon_7$  like  $\epsilon_5$ . The transitions  $\epsilon_{-i}$ ,  $i = 4, 5, 6, 7$ , represent reverse processes. The equations are more compactly written if we index the state by integer numbers:  $q_1 = E2F1, q_2 = DP1, q_3 = pRb, q_4 = a, q_5 = b, q_6 = c, q_7 = d, q_8 = mRNA$ . The time evolution for  $X(z, t)$  is given by:



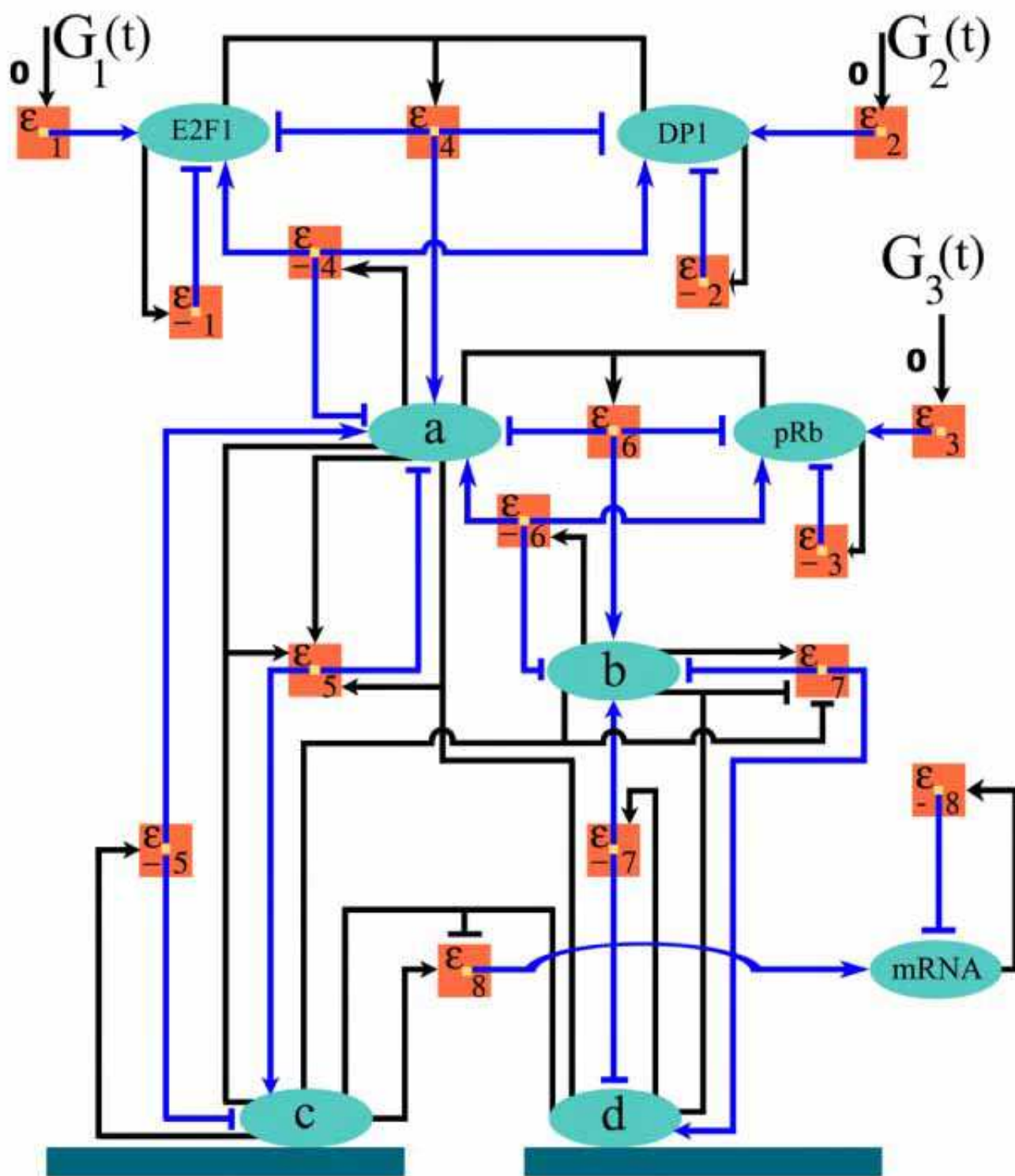


FIG. 14: Molecular diagram for E2F1 regulatory element.

$$\begin{aligned}
\partial_t X &= G_1(t)(z_1 - 1) + k_{-1}(1 - z_1)\partial_1 X \\
&+ G_2(t)(z_2 - 1) + k_{-2}(1 - z_2)\partial_2 X \\
&+ G_3(t)(z_3 - 1) + k_{-3}(1 - z_3)\partial_3 X \\
&+ k_4(z_4 - z_1 z_2)(\partial_{12} X + \partial_1 X \partial_2 X) + k_{-4}(z_1 z_2 - z_4)\partial_4 X \\
&+ k_5(z_6 - z_4)(n_1 \partial_4 X - n_2 z_6(\partial_{46} X + \partial_4 X \partial_6 X) - n_3 z_7(\partial_{47} X + \partial_4 X \partial_7 X)) \\
&+ k_{-5}(z_4 - z_6)\partial_6 X \\
&+ k_6(z_5 - z_3 z_4)(\partial_{34} X + \partial_3 X \partial_4 X) + k_{-6}(z_3 z_4 - z_5)\partial_5 X \\
&+ k_7(z_7 - z_5)(m_1 \partial_5 X - m_2 z_6(\partial_{56} X + \partial_5 X \partial_6 X) - m_3 z_7(\partial_{57} X + \partial_5 X \partial_7 X)) \\
&+ k_{-7}(z_5 - z_7)\partial_7 X \\
&+ k_8(z_6 z_8 - z_6)(l_1 \partial_6 X - l_2 z_7(\partial_{67} X + \partial_6 X \partial_7 X)) \\
&+ k_{-8}(1 - z_8)\partial_8 X.
\end{aligned} \tag{II.34}$$

The equations for the mean of the state components are:

$$\begin{aligned}
\dot{X}_1 &= G_1(t) - k_{-1}X_1 - k_4(X_{12} + X_1X_2) + k_{-4}X_4, \\
\dot{X}_2 &= G_2(t) - k_{-2}X_2 - k_4(X_{12} + X_1X_2) + k_{-4}X_4, \\
\dot{X}_3 &= G_3(t) - k_{-3}X_3 - k_6(X_{34} + X_3X_4) + k_{-6}X_5, \\
\dot{X}_4 &= k_4(X_{12} + X_1X_2) - k_{-4}X_4 - k_5(n_1X_4 - n_2(X_{46} + X_4X_6) - n_3(X_{47} + X_4X_7)) \\
&+ k_{-5}X_6 - k_6(X_{34} + X_3X_4) + k_{-6}X_5, \\
\dot{X}_5 &= k_6(X_{34} + X_3X_4) - k_{-6}X_5 - k_7(m_1X_5 - m_2(X_{56} + X_5X_6) - M_3(X_{57} + X_5X_7)) + k_{-7}X_7, \\
\dot{X}_6 &= k_5(n_1X_4 - n_2(X_{46} + X_4X_6) - n_3(X_{47} + X_4X_7)) - k_{-5}X_6, \\
\dot{X}_7 &= k_7(m_1X_5 - m_2(X_{56} + X_5X_6) - m_3(X_{57} + X_5X_7)) - k_{-7}X_7, \\
\dot{X}_8 &= k_8(l_1X_6 - l_2(X_{67} + X_6X_7)) - k_{-8}X_8.
\end{aligned} \tag{II.35}$$

As in the previous examples, the system of equations is infinite because in the equation for an  $X_m$ , variables  $X_{m'}$  with higher order indices  $m' > m$  are present. For example, to compute the standard deviation of the the mRNA number, we need to include the following equation in the system

$$\dot{X}_{88} = 2k_8(l_1X_{68} - l_2(X_{678} + X_6X_{78} + X_{68}X_7)) - 2k_{-8}X_{88}, \tag{II.36}$$

which contains the third order variable  $X_{678}$ . Because the state has 8 components, there will be a total of 164 equations for the  $X_m(t)$  variables, up to third order in  $m$  ( $|m| \leq 3$ ). We will disregard any fourth order variables in the following, so that we will work with a set of 164 equations. Again, the constant part of the generators  $G_1, G_2$  and  $G_3$  will fix a stationary state. The equations for the stationary point are polynomial in  $X_{m,0}$ , and thus can be solved by using one of the existing algorithms for polynomial systems of equations [44]. The system is large and many unphysical solutions will be generated by solving it directly. A strategy to obtain the desired solution is to use at the beginning only the equations for the first order cumulants where we set all higher order factorial cumulants equal to zero. This partial solution will be used as a starting point for finding a solution for the entire 164 equations. For the following set of parameters:  $\{G_1 = 340, G_2 = 275, G_3 = 2.86, k_4 = 1, k_{-3} = 0.13, k_{-6} = 3.025, k_{-4} = 10, k_5 = 14, l_1 = 60, k_{-7} = 7.773, k_{-1} =$

17,  $k_{-2} = 11$ ,  $k_8 = 1$ ,  $k_6 = 0.11$ ,  $k_7 = 0.011$ ,  $k_{-8} = 22.800$ ,  $k_{-5} = 9275$ ,  $n_1 = 60$ ,  $n_2 = 1$ ,  $n_3 = 1$ ,  $m_1 = 60$ ,  $m_2 = 1$ ,  $m_3 = 1$ ,  $l_1 = 60$ ,  $l_2 = 1$ }, the stationary point for the mean values of the state is  $\{X_{1,0} = 20, X_{2,0} = 25, X_{3,0} = 22, X_{4,0} = 50, X_{5,0} = 40, X_{6,0} = 4, X_{7,0} = 3, X_{8,0} = 10\}$ . We notice that the constraints imposed upon the transition probabilities were effective in the sense that the values for the molecules  $c$  and  $d$  that bind to the DNA are much less than the values for the unbound molecules  $a$  and  $b$ . Out of the 164 values for the  $X_{m,0}$  at the stationary point, the maximum value is  $X_{48,0} = 6.88$  which expresses the correlation between the mRNA and the dimer  $a$ . The minimum negative number is  $X_{78,0} = -0.73$ , for the correlation between mRNA and the DNA-bound molecule  $d$ . The generators will modulate the mRNA level through their time dependant term  $g_i(t)$ ,  $i = 1, 2, 3$ . The effect of these input variations can be computed like we did in the previous examples, using an expansion in the small parameter  $\eta$ . Then the mRNA level will vary according to

$$\begin{aligned} X_{8,1}(s) &= H_8^1(s)g_1(s) + H_8^2(s)g_2(s) + H_8^3(s)g_3(s) , \\ X_{88,1}(s) &= H_{88}^1(s)g_1(s) + H_{88}^2(s)g_2(s) + H_{88}^3(s)g_3(s) , \end{aligned} \quad (\text{II.37})$$

were the transfer functions are

$$\begin{aligned} H_8^1(s) &= \frac{0.06 s^2 + 0.65 s + 0.87}{(s + 1.57)(s + 1.48)(s + 1.38)} , & H_{88}^1(s) &= \frac{0.0002 s^2 + 0.0228 s + 0.0340}{(s + 80.9)(s + 1.57)(s + 1.48)} , \\ H_8^2(s) &= \frac{0.01 s^2 + 0.18 s + 0.26}{(s + 1.57)(s + 1.48)(s + 3.79)} , & H_{88}^2(s) &= \frac{0.01 s^2 + 0.14 s + 0.29}{(s + 1.57)(s + 11.30)(s + 3.01)} , \\ H_8^3(s) &= \frac{-0.16 s^2 - 2.16 s - 0.52}{(s + 0.043)(s + 1.48)(s + 22.8)} , & H_{88}^3(s) &= \frac{0.006 s^2 - 0.066 s - 0.023}{(s + 1.57)(s + 13.08)(s + 0.043)} . \end{aligned}$$

The transfer functions obtained from all 164 equations are actually rational functions of much higher powers than those above. The inverse Laplace transform of these solutions consists of a sum of many exponential decaying components. Some components are very small, so they can be neglected. We did an exhaustive search through all groups of 3 components to find the best approximation. The error was computed as the ratio of the  $L_2$  norm of the difference between the solution and its approximation, over the  $L_2$  norm of the solution. The average error for the formulas above is 6%. Using more than 3 decaying components to approximate the transfer function will decrease the error, but will increase the complexity of the rational function. From the expression of the transfer function  $H_8^3$ , we see that the pRb acts with a negative sign, as was expected. However, the relative strength of the action of each signal generator on the mRNA level can not be assessed unless we solve the dynamical equations.

### III. TIME EVOLUTION EQUATION FOR A GENE REGULATORY NETWORK EXCITED BY SIGNAL GENERATORS

The systems studied in the previous sections proved the usefulness of the equations for the variables  $X_m(t)$  and showed how to use these equations to solve practical problems. Now we aim to write the time evolution equation for  $X_m(t)$  for a general stochastic nonlinear regulatory network. Nonlinear refers here to transition probabilities that are rational functions in the state variables. A genetic regulatory network is represented by a vector  $q = (q_1, \dots, q_n)$ . Each  $q_i$  represent the number of molecules for the component  $i$  of the state  $q$ . The components  $i = 1 \dots n$  can represent different proteins, mRNAs, or the same protein but in different configurations or localizations (in nucleus,

on the membrane, in Golgi apparatus etc.). The state components  $q_i$  change in time due to a set of possible transitions  $\epsilon$ . If at time  $t$  the state is  $q$ , then at time  $t + dt$  the state will be  $q + \epsilon$ , with  $\epsilon$  one of the possible transitions. Each transition is governed by its probability of transition  $T_\epsilon(q, t)$  which depends on the state variables  $q$  and time  $t$ . To express this state dependance we need some notations.

A vector  $\bar{m} = (m_1, m_2, \dots, m_n)$  will index a set of polynomials which will constitute a basis for the set of all polynomials in  $q$ :

$$e_{\bar{m}}(q) = e_{m_1}(q_1) \dots e_{m_n}(q_n) \quad (\text{III.1})$$

with

$$e_{m_k}(q_k) = q_k(q_k - 1) \dots (q_k - m_k + 1). \quad (\text{III.2})$$

The  $e_{m_k}$  is known as the falling factorial and is related with the Pochhammer symbol. We will refer to  $e_{\bar{m}}(q)$  as the factorial basis. Each vector  $\bar{m}$  can be written in a tensor notation

$$m = \underbrace{11\dots 1}_{m_1} \underbrace{22\dots 2}_{m_2} \dots \underbrace{nn\dots n}_{m_n} \quad (\text{III.3})$$

and each tensor index  $m$  can be transferred into a vector notation  $\bar{m}$ . The modulus of  $m$  or  $\bar{m}$  is the degree of the polynomial:  $|m| \equiv |\bar{m}| = \sum_{k=1}^n m_k$ .

To find the standard deviations or moments of the state  $q$ , the transformation between the factorial basis and the basis  $\{1, x, x^2, \dots, x^l \dots\}$  is helpful

$$x^l = \sum_{k=0}^l S(l, k) e_k(x), \quad (\text{III.4})$$

where  $S(l, k)$  are the Stirling numbers of the second kind. The inverse transformation depends on the Stirling numbers of the first kind  $s(l, k)$

$$e_l(x) = \sum_{k=0}^l s(l, k) x^k. \quad (\text{III.5})$$

In general,

$$e_{\bar{m}}(q) = \prod_{i=1}^n e_{\bar{m}_i}(q_i) = \prod_{i=1}^n \sum_{k_i=0}^{m_i} s(m_i, k_i) q_i^{k_i} = \sum_{\bar{k}=0}^{\bar{m}} \prod_{i=1}^n s(m_i, k_i) q_i^{k_i}; \quad (\text{III.6})$$

therefore

$$\langle e_{\bar{m}}(q) \rangle = \sum_{\bar{k}=0}^{\bar{m}} s(m_1, k_1) s(m_2, k_2) \dots s(m_n, k_n) \langle q_1^{k_1} q_2^{k_2} \dots q_n^{k_n} \rangle \quad (\text{III.7})$$

and

$$\langle q_1^{m_1} q_2^{m_2} \dots q_n^{m_n} \rangle = \sum_{\bar{k}=0}^{\bar{m}} S(m_1, k_1) S(m_2, k_2) \dots S(m_n, k_n) \langle e_{\bar{k}}(q) \rangle . \quad (\text{III.8})$$

With the help of the factorial basis we can write 3 types of transition probabilities, linear transition:

$$T_\epsilon(q, t) = \sum_k M_\epsilon^k(t) q_k , \quad (\text{III.9})$$

polynomial transition:

$$T_\epsilon(q, t) = \sum_m M_\epsilon^m(t) e_{\bar{m}}(q) , \quad (\text{III.10})$$

and rational transition:

$$T_\epsilon(q, t) = \frac{\sum_m M_\epsilon^m(t) e_{\bar{m}}(q)}{\sum_n M_\epsilon^n(t) e_{\bar{n}}(q)} . \quad (\text{III.11})$$

To keep the components of the state  $q$  positive or zero the transition probabilities should obey some boundary conditions. The state with at least one component set on zero is on the boundary of the set of all possible states. On the boundary, some of the  $\epsilon$ 's will point outside, and there is a danger that the system will jump into a state with at least one state component with negative molecule numbers. To avoid the unphysical negative states, we will impose boundary conditions on the transition probabilities. Consider a system that is in a positive state at  $t = 0$ . This system will never jump in a negative region if  $T_\epsilon(q, t) = 0$  for  $q_i$  such that  $q_i + \epsilon_i \leq -1$ ,  $i = 1, \dots, n$ . The last inequality can be expressed in terms of  $\bar{m}$  if we look at the structure of the transition probability  $T_\epsilon(q, t) = \sum_m M_\epsilon^m(t) e_{\bar{m}}(q)$  and the roots of  $e_{\bar{m}}(q)$ . Namely, the condition  $q_i + \epsilon_i \leq -1$ ,  $i = 1, \dots, n$  is fulfilled if

$$\bar{m} \geq -\epsilon \quad (\text{III.12})$$

for every  $m$  in  $T_\epsilon(q, t)$  with  $M_\epsilon^m(t) \neq 0$ . The boundary condition (III.12) for rational transition probabilities refers to the numerator of (III.11).

We will first deduce the time variation equation for the polynomial transitions:

$$T_\epsilon(q, t) = \sum_m M_\epsilon^m(t) \mathbf{e}_{\bar{m}}(q) . \quad (\text{III.13})$$

To excite a gene regulatory network, an experimental scientist must act on it through a set of signal generators. The signal generators are present in the coefficients  $M_\epsilon^m(t)$ . The most obvious way to introduce a signal generator is by adding it to a transition probability

$$T_\epsilon(q, t) = \sum_m M_\epsilon^m e_{\bar{m}}(q) + G(t) . \quad (\text{III.14})$$

Written in the factorial basis the generator is  $G(t) = M_\epsilon^0(t) e_0(q)$ . This type of signal generator can be implemented using a light switch to control the promoter of a gene, Fig. 2. A different

type of signal generator modulates protein degradation. An experimental implementation of such a generator will have a tremendous impact on the protein function prediction. The influence of such a generator can be written as

$$T_\epsilon(q, t) = \sum_m M_\epsilon^m e_{\bar{m}}(q) + G(t) e_{\bar{\pi}}(q) \quad (\text{III.15})$$

where  $G(t) = M_\epsilon^n(t)$ , with  $n \geq -\epsilon$  to satisfy the boundary conditions.

The equation for the probability of the gene regulatory network  $P(q_1, \dots, q_n, t)$  to be in the state  $q$  at time  $t$  is

$$\frac{\partial P(q, t)}{\partial t} = \sum_\epsilon T_\epsilon(q - \epsilon, t) P(q - \epsilon, t) - \sum_\epsilon T_\epsilon(q, t) P(q, t). \quad (\text{III.16})$$

We are interested in the mean values for different molecules, as well as their correlations. The generating function for such variables is  $F(z, t)$  which is the  $\mathcal{Z}$ -transform of  $P(q, t)$ :

$$F(z, t) \equiv \mathcal{Z}(P(q, t)) = \sum_q z^q P(q, t). \quad (\text{III.17})$$

Here  $z = (z_1, \dots, z_n)$  and  $z^q = z_1^{q_1} \dots z_n^{q_n}$ .

Taking care of the boundary condition (III.12), the equation for the variable  $F(z, t)$  is

$$\frac{\partial F}{\partial t} = \sum_{\epsilon, m} (z^{\epsilon + \bar{m}} - z^{\bar{m}}) M_\epsilon^m(t) \partial_m F \quad (\text{III.18})$$

where we used the property that

$$\mathcal{Z}(e_{\bar{m}}(q) P(q, t)) = z^{\bar{m}} \partial_m F(z, t). \quad (\text{III.19})$$

The variables that describe the dynamic of the system are generated by taking partial derivatives of  $F(z, t)$  with respect to  $z$ . For this process the following relation is useful:

$$\partial_\alpha(z^\epsilon) = Q_\alpha(\epsilon) z^{\epsilon - \bar{\alpha}}, \quad (\text{III.20})$$

with

$$Q_\alpha(\epsilon) = \epsilon_\alpha. \quad (\text{III.21})$$

In what follows, the Greek letters will refer to a one dimensional index that runs from 1 to  $n$ . The Latin letters will refer to a tensor index  $m = \alpha_1 \alpha_2 \alpha_3 \dots$ . Then  $\partial_{\alpha\beta}(z_1^{\epsilon_1} \dots z_n^{\epsilon_n}) = \partial_\beta(Q_\alpha(\epsilon) z^{\epsilon - \bar{\alpha}}) = Q_{\alpha\beta}(\epsilon) z^{\epsilon - \bar{\alpha} - \bar{\beta}}$ , with  $Q_{\alpha\beta}(\epsilon) = Q_\alpha(\epsilon) Q_\beta(\epsilon - \bar{\alpha})$ .

In general

$$\partial_m z^\epsilon = Q_m(\epsilon) z^{\epsilon - \bar{m}},$$

with

$$Q_{m\alpha}(\epsilon) = Q_m(\epsilon) Q_\alpha(\epsilon - \bar{m}).$$

From (III.18) we obtain

$$\partial_\alpha \dot{F} = \sum_{m,\epsilon} (Q_\alpha(\epsilon + \bar{m})z^{\epsilon + \bar{m} - \bar{\alpha}} - Q_\alpha(\bar{m})z^{\bar{m} - \bar{\alpha}})M_\epsilon^m(t)\partial_m F + \sum_{m,\epsilon} (z^{\epsilon + \bar{m}} - z^{\bar{m}})M_\epsilon^m(t)\partial_{m\alpha} F$$

and for  $z = 1$

$$\dot{F}_\alpha = \sum_{m,\epsilon} (Q_\alpha(\epsilon + \bar{m}) - Q_\alpha(\bar{m}))M_\epsilon^m(t)F_m. \quad (\text{III.22})$$

With the compact notation

$$R_\alpha^m(t) = \sum_{\epsilon} (Q_\alpha(\epsilon + \bar{m}) - Q_\alpha(\bar{m}))M_\epsilon^m(t), \quad (\text{III.23})$$

the equation (III.22) becomes

$$\dot{F}_\alpha = R_\alpha^m(t)F_m, \quad (\text{III.24})$$

where summation over the dummy index  $m$  is implied.

Similarly:

$$\dot{F}_{\alpha\beta} = R_{\alpha\beta}^m(t)F_m + R_\alpha^m(t)F_{m\beta} + R_\beta^m(t)F_{m\alpha}, \quad (\text{III.25})$$

with

$$R_{\alpha\beta}^m(t) = \sum_{\epsilon} (Q_{\alpha\beta}(\epsilon + \bar{m}) - Q_{\alpha\beta}(\bar{m}))M_\epsilon^m(t). \quad (\text{III.26})$$

The general equations for the  $F_m$  variables are obtained by applying the operator  $\partial_{\alpha_1 \dots \alpha_n}$  to (III.18). We write the action of this operator on a product of two functions as:

$$\partial_{\alpha_1 \dots \alpha_n} (fg) = \left\{ \partial_{\alpha_1 \dots \alpha_k} f \partial_{\alpha_{k+1} \dots \alpha_n} g \right\}_\alpha, \quad (\text{III.27})$$

where the braces indicate the summation for all pairs of disjoint sets  $(\alpha_1 \dots \alpha_k), (\alpha_{k+1} \dots \alpha_n)$  that form a partition of the tensor index  $\alpha_1 \dots \alpha_n$ . When listing all possible partitions, we take care that a permutation of the elements of a set does not change said set. Also  $R^m$  with an empty index set is zero, because  $Q(\epsilon) = 1$ , which comes from  $z^\epsilon = Q(\epsilon)z^\epsilon$ , see (III.20).

Then the equation for the time variation of  $F_m(t)$  is

$$\dot{F}_{\alpha_1 \dots \alpha_n} = \left\{ R_{\alpha_1 \dots \alpha_k}^m(t) F_{m\alpha_{k+1} \dots \alpha_n} \right\}_\alpha, \quad (\text{III.28})$$

where summation over the dummy index  $m$  is implied. The tensor  $R_{\alpha_1 \dots \alpha_k}^m(t)$  is given by (III.26) with  $\alpha_1 \dots \alpha_k$  instead of the index  $\alpha\beta$ . To see the structure of the equation (III.28) we specialize it for  $n = 3$ .

$$\begin{aligned} \dot{F}_{\alpha_1 \alpha_2 \alpha_3} &= R_{\alpha_1 \alpha_2 \alpha_3}^m(t)F_m \\ &+ R_{\alpha_1 \alpha_2}^m(t)F_{m\alpha_3} + R_{\alpha_1 \alpha_3}^m(t)F_{m\alpha_2} + R_{\alpha_2 \alpha_3}^m(t)F_{m\alpha_1} \\ &+ R_{\alpha_1}^m(t)F_{m\alpha_2 \alpha_3} + R_{\alpha_2}^m(t)F_{m\alpha_1 \alpha_3} + R_{\alpha_3}^m(t)F_{m\alpha_1 \alpha_2}. \end{aligned} \quad (\text{III.29})$$

### A. Factorial Cumulants and Filled Young Tableaux

The equation (III.28) has a similar structure with what is called a bilinear system in Nonlinear Control Theory. A bilinear system is represented by a time evolution equation that is linear in state, linear in control, but not jointly linear in both

$$\frac{dx}{dt} = Ax + \sum_{k=1}^n N_k u_k x + Bu, \quad (\text{III.30})$$

where  $x \in \mathbb{R}^n$  and  $A, N_k, k = 1 \dots n, B$  are appropriate matrices [45]. The controls are  $u_k, k = 1 \dots n$  and the state is described by  $x$ . However, the system (III.28) is not finite like (III.30), and as we explained in the first section, discarding  $F_m$  with higher order  $m$  will produce an unstable finite system of equations. Our goal is twofold: (1) to change the variables  $F_m$  so that the discarding process for obtaining a finite number of equations become meaningful and (2) to keep the bilinear structure of the equations in the new variable.

The change of variable:

$$F(z, t) = e^{X(z, t)} \quad (\text{III.31})$$

is similar with the change from moments to cumulants [36]. Because  $F(z, t)$  generates the factorial moments,  $X(z, t)$  will generate the factorial cumulants.

The time dependent variables,  $F_m$ , will be replaced by  $X_m = \partial_m X(z, t) |_{z=1}$ . The transformation relations between  $F_m$  and  $X_m$  follow from the Faà Di Bruno's formula for the derivative of the composition of functions [46]. To keep the bilinear structure, we need to construct an appropriate index notation for the terms of the Faà Di Bruno's formula. We introduce the index construction by way of an example. The fourth order derivative of  $F$  at  $z = 1$  is

$$\begin{aligned} F_{\alpha\beta\gamma\delta} = & X_{\alpha\beta\gamma\delta} + \\ & X_{\alpha\beta\gamma}X_{\delta} + X_{\alpha\beta\delta}X_{\gamma} + X_{\alpha\gamma\delta}X_{\beta} + X_{\beta\gamma\delta}X_{\alpha} + \\ & X_{\alpha\beta}X_{\gamma\delta} + X_{\alpha\gamma}X_{\beta\delta} + X_{\alpha\delta}X_{\beta\gamma} + \\ & X_{\alpha\beta}X_{\gamma}X_{\delta} + X_{\alpha\gamma}X_{\beta}X_{\delta} + X_{\alpha\delta}X_{\beta}X_{\gamma} + X_{\beta\gamma}X_{\alpha}X_{\delta} + X_{\beta\delta}X_{\alpha}X_{\gamma} + X_{\gamma\delta}X_{\alpha}X_{\beta} + \\ & X_{\alpha}X_{\beta}X_{\gamma}X_{\delta} \end{aligned} \quad (\text{III.32})$$

Given the index  $\alpha\beta\gamma\delta$  from the left side of (III.32) we need to generate all the indices that appear in the right side of (III.32). If the term  $X_{\alpha\gamma}X_{\beta}X_{\delta}$  is present in the sum, then any symmetric version of it, like  $X_{\beta}X_{\gamma\alpha}X_{\delta}$ , cannot be present. If we classify all possible symmetries of a term, then we will find an index notation that will eliminate all the equivalent terms. The symmetries come from the commutativity of the product and the commutativity of the partial derivatives. Young tableaux and filled Young tableaux will help to classify the symmetries and also to construct an index notation which will keep the bilinear structure. A Young tableau is associated with a partition of an integer  $N$ . For a fixed positive integer  $N$ , to each partition  $N = \mu_1\lambda_1 + \mu_2\lambda_2 + \dots + \mu_k\lambda_k$ ,  $\lambda_1 > \lambda_2 > \dots > \lambda_k > 0$ , we associate an empty Young tableau consisting of  $\mu_i$  rows of  $\lambda_i$  empty boxes,  $i = 1, \dots, k$ . For example consider the partition  $8 = 3 + 2 + 2 + 1 = 3 + 2 \cdot 2 + 1$ , that is  $\mu_1 = 1, \lambda_1 = 3, \mu_2 = 2, \lambda_2 = 2, \mu_3 = 1, \lambda_3 = 1$ . The Young tableau corresponding to this partition is

$$Y = \begin{array}{|c|c|c|} \hline \square & \square & \square \\ \hline \square & \square & \\ \hline \square & \square & \\ \hline \square & & \\ \hline \end{array}$$



We will use these Young tableaux filled with indices  $\alpha, \beta, \gamma, \dots$ , to represent products of  $X_m$  variables:

$$X_{\begin{array}{|c|c|c|} \hline \alpha & \beta & \gamma \\ \hline \delta & & \\ \hline \end{array}} = X_{\alpha\beta\gamma} X_{\delta}$$

Then (III.32) is written using filled Young tableaux as indices as follows:

$$\begin{aligned} F_{\begin{array}{|c|c|c|c|} \hline \alpha & \beta & \gamma & \delta \\ \hline \end{array}} &= X_{\begin{array}{|c|c|c|c|} \hline \alpha & \beta & \gamma & \delta \\ \hline \end{array}} + \\ &X_{\begin{array}{|c|c|c|} \hline \alpha & \beta & \gamma \\ \hline \delta & & \end{array}} + X_{\begin{array}{|c|c|c|} \hline \alpha & \beta & \delta \\ \hline \gamma & & \end{array}} + X_{\begin{array}{|c|c|c|} \hline \alpha & \gamma & \delta \\ \hline \beta & & \end{array}} + X_{\begin{array}{|c|c|c|} \hline \beta & \gamma & \delta \\ \hline \alpha & & \end{array}} + \\ &X_{\begin{array}{|c|c|} \hline \alpha & \beta \\ \hline \gamma & \delta \end{array}} + X_{\begin{array}{|c|c|} \hline \alpha & \gamma \\ \hline \beta & \delta \end{array}} + X_{\begin{array}{|c|c|} \hline \alpha & \delta \\ \hline \beta & \gamma \end{array}} + \\ &X_{\begin{array}{|c|c|} \hline \alpha & \beta \\ \hline \gamma & \delta \end{array}} + X_{\begin{array}{|c|c|} \hline \alpha & \gamma \\ \hline \beta & \delta \end{array}} + X_{\begin{array}{|c|c|} \hline \alpha & \delta \\ \hline \beta & \gamma \end{array}} + X_{\begin{array}{|c|c|} \hline \beta & \gamma \\ \hline \alpha & \delta \end{array}} + X_{\begin{array}{|c|c|} \hline \beta & \delta \\ \hline \alpha & \gamma \end{array}} + X_{\begin{array}{|c|c|} \hline \gamma & \delta \\ \hline \alpha & \beta \end{array}} + \\ &X_{\begin{array}{|c|} \hline \alpha \\ \hline \beta \\ \hline \gamma \\ \hline \delta \end{array}} \end{aligned}$$

The rows of a Young tableau are listed in decreasing order of their length, which will enforce an order in the product of the variables  $X_m$ . Thus the symmetry due to the commutativity of the product is lifted. However, in a block of rows of equal length there is still an ambiguity in ordering the terms in a product. To lift the ambiguity, we will order rows of equal length in decreasing lexicographic order of the words that are placed in rows. For example, in the 6th term of the above formula  $\alpha\beta > \gamma\delta$  and thus  $\alpha\beta$  is placed above  $\gamma\delta$ . The lexicographic order between the tensor indices is induced by the order of the components of the state:  $q_i < q_j$  if  $i < j$ . There is one more symmetry left to be lifted. This symmetry is generated by the commutativity of the partial derivatives and is lifted by ordering the letters in a row from left to right. For example, the 4th term in the formula above has  $\alpha\gamma\delta$  on its first row and not  $\gamma\alpha\delta$ . Mathematically, the symmetries are described with the help of a set of permutations that act on the tensor index that fill a Young tableau. The components of a tensor index  $m$  will be denoted using superscripts not to be confused with the components of the vector  $\bar{m}$ ; thus  $m = m^1 m^2 m^3 \dots$ . A Young tableau  $Y$  filled with a tensor index  $m$  from  $F_m$  is denoted by  $Y[m]$ . The filling process starts from the upper left box of  $Y$  where  $m^1$  is inserted, and moves from left to right and top to bottom. The action of a permutation  $\sigma$  on the elements of  $Y[m]$  is denoted by  $Y[m^\sigma]$  and is exemplified below:

$$Y[m] = \begin{array}{|c|c|c|} \hline m^1 & m^2 & m^3 \\ \hline m^4 & & \\ \hline \end{array} \qquad Y[m^\sigma] = \begin{array}{|c|c|c|} \hline m^{\sigma(1)} & m^{\sigma(2)} & m^{\sigma(3)} \\ \hline m^{\sigma(4)} & & \\ \hline \end{array}$$

For example, if  $Y = \begin{array}{|c|c|c|} \hline & & \\ \hline & & \\ \hline \end{array}$ ,  $m = \alpha\beta\gamma\delta$ ,  $\sigma(1) = 1, \sigma(2) = 2, \sigma(3) = 4$  and  $\sigma(4) = 3$  we have:

$$Y[m] = \begin{array}{|c|c|c|} \hline \alpha & \beta & \gamma \\ \hline \delta & & \\ \hline \end{array} \qquad Y[m^\sigma] = \begin{array}{|c|c|c|} \hline \alpha & \beta & \delta \\ \hline \gamma & & \\ \hline \end{array}$$

and

$$X_{Y[m]} = X_{\alpha\beta\gamma}X_{\delta} \quad (\text{III.33})$$

$$X_{Y[m^\sigma]} = X_{\alpha\beta\delta}X_{\gamma}. \quad (\text{III.34})$$

To lift the last symmetry, we need to find the permutations  $\sigma$  which leave the term  $X_{Y[m]}$  invariant, that is  $X_{Y[m^\sigma]} = X_{Y[m]}$ . In general, the components  $m^i$  of the tensor index  $m$  need not be distinct. For example we have  $m=rpp$  in (II.18). However, to obtain the Faà Di Bruno formula, when we solve for  $\sigma$  in  $X_{Y[m^\sigma]} = X_{Y[m]}$ , the index  $m$  must have distinct components ( $m^i \neq m^j$  for all  $i \neq j$ ). The set of permutations  $\sigma$  thus found form a subgroup of the permutation group  $S_{|Y|}$ . Here  $|Y|$  is the dimension of the Young tableau  $Y$  which equals the total number of its boxes. This subgroup is denoted as  $H^Y$ .

The terms in the Faà Di Bruno formula will be generated using filled Young tableaux and a set of representative permutations  $\sigma_i, i = 1 \dots J$  chosen from each set of the coset space

$$S_{|Y|}/H^Y = \{\sigma_1 H^Y, \dots, \sigma_J H^Y\}. \quad (\text{III.35})$$

Here  $J$  is  $|Y|!/\text{cardinal}(H^Y)$ . The lexicographic order is a practical method to select a set of representative permutations  $\sigma_1, \dots, \sigma_J$ , without computing the invariant subgroup  $H^Y$  and the coset space; we will use the lexicographic order for simple cases. However, for general results we will use the coset space. Some examples of invariant subgroups and coset spaces are presented in Table 4.

**TABLE 6: Subgroups and Coset Spaces**

$Y[\alpha\beta\gamma\delta]$	$H^Y$	$S_{ Y }/H^Y$
$\begin{array}{ c c c c } \hline \alpha & \beta & \gamma & \delta \\ \hline \end{array}$	$S_4$	$\{(1)\}$
$\begin{array}{ c c c } \hline \alpha & \beta & \gamma \\ \hline \delta & & \\ \hline \end{array}$	$\{(123), (12)\}$	$\{(1), (34), (24), (14)\}$
$\begin{array}{ c c } \hline \alpha & \beta \\ \hline \gamma & \delta \\ \hline \end{array}$	$\{(12), (34), (13)(24)\}$	$\{(1), (23), (243)\}$
$\begin{array}{ c c } \hline \alpha & \beta \\ \hline \gamma & \\ \hline \delta & \\ \hline \end{array}$	$\{(12), (34), (12)(34)\}$	$\{(1), (23), (24), (13), (14), (13)(24)\}$
$\begin{array}{ c } \hline \alpha \\ \hline \beta \\ \hline \gamma \\ \hline \delta \\ \hline \end{array}$	$S_4$	$\{(1)\}$

In the above table we used the cycle notation for permutations: (123) means  $\sigma(1) = 2, \sigma(2) = 3, \sigma(3) = 1$ .

Finally we can write the Faà Di Bruno formula in Young tableaux notation:

$$F_m = \sum_{|Y|=|m|} \sum_{\sigma \in S_{|Y|}/H^Y} X_{Y[m^\sigma]} . \quad (\text{III.36})$$

Here the tensor index  $m$  can have any form; there is no need for the components  $m^i$  to be distinct (as it was when we defined  $H^Y$ ).

For partial derivatives with  $z$  not fixed to 1 the formula is similar

$$\partial_m F(z, t) = \sum_{|Y|=|m|} \sum_{\sigma \in S_{|Y|}/H^Y} \partial_{Y[m^\sigma]} X(z, t) e^{X(z, t)} , \quad (\text{III.37})$$

with the convention that the derivation, with respect to a filled Young tableau, is the product of the derivatives along each line of the tableau. Thus, using the example (III.33) we have:

$$\partial_{Y[m]} X(z, t) = \partial_\alpha \partial_\beta \partial_\gamma X(z, t) \partial_\delta X(z, t) . \quad (\text{III.38})$$

## B. Equation of Motion for Polynomial Transition Probabilities

The equation (III.18) in the variable  $X(z, t)$  is

$$\partial_t X(z, t) = \sum_{m, \epsilon} (z^{\epsilon + \bar{m}} - z^{\bar{m}}) M_\epsilon^m(t) \left[ \sum_{|Y|=|m|} \sum_{\sigma \in S_{|Y|}/H^Y} \partial_{Y[m^\sigma]} X(z, t) \right] . \quad (\text{III.39})$$

The time dependent variables will now be  $\partial_m X(z, t) |_{z=1}$ , so that we must take partial derivatives with respect to  $z$  of (III.39). The concatenation notation  $\partial_{\alpha\beta} = \partial_\alpha \partial_\beta$  must be generalized for filled Young tableaux

$$\partial_{\alpha|Y[m]} X(z, t) := \partial_\alpha (\partial_{Y[m]} X(z, t)) . \quad (\text{III.40})$$

From the definition (III.40), the concatenation  $\alpha|Y[m]$  means that a box containing  $\alpha$  must be glued to each row of  $Y[m]$  and the object thus obtained must be rearranged into a lexicographical order filled Young tableau. Here is an example of concatenation with a box filled with the index 2:

$$\partial_2 (\partial_{\begin{array}{|c|c|c|} \hline 1 & 2 & 3 \\ \hline 4 & 5 \\ \hline 6 & 7 \\ \hline 8 \\ \hline \end{array}} X(z, t)) = \partial_{\begin{array}{|c|c|c|c|} \hline 1 & 2 & 2 & 3 \\ \hline 4 & 5 \\ \hline 6 & 7 \\ \hline 8 \\ \hline \end{array}} X(z, t) + \partial_{\begin{array}{|c|c|c|} \hline 1 & 2 & 3 \\ \hline 2 & 4 & 5 \\ \hline 6 & 7 \\ \hline 8 \\ \hline \end{array}} X(z, t) + \partial_{\begin{array}{|c|c|c|} \hline 1 & 2 & 3 \\ \hline 2 & 6 & 7 \\ \hline 4 & 5 \\ \hline 8 \\ \hline \end{array}} X(z, t) + \partial_{\begin{array}{|c|c|c|} \hline 1 & 2 & 3 \\ \hline 4 & 5 \\ \hline 6 & 7 \\ \hline 2 & 8 \\ \hline \end{array}} X(z, t)$$

Inductively we define

$$\partial_{\alpha|\beta|\dots|\gamma|Y[m]} = \partial_\alpha (\partial_{\beta|\dots|\gamma|Y[m]}) . \quad (\text{III.41})$$

The concatenation notation will be also applied to the  $X_m$  variable:

$$X_{\alpha|Y[m]} := \partial_{\alpha|Y[m]} X(z, t) |_{z=1} .$$

The equations for the factorial cumulants are now a consequence of (III.39)

$$\dot{X}_\alpha = R_\alpha^m(t) \sum_{Y,\sigma} X_{Y[m^\sigma]}, \quad (\text{III.42})$$

$$\dot{X}_{\alpha\beta} = R_{\alpha\beta}^m(t) \sum_{Y,\sigma} X_{Y[m^\sigma]} + R_\alpha^m(t) \sum_{Y,\sigma} X_{\beta|Y[m^\sigma]} + R_\beta^m(t) \sum_{Y,\sigma} X_{\alpha|Y[m^\sigma]}, \quad (\text{III.43})$$

with  $\sum_{Y,\sigma}$  being a short notation for the the sums over  $Y$  and  $\sigma$  in (III.39).  
In general

$$\dot{X}_{\alpha_1\alpha_2\dots\alpha_n} = \left\{ R_{\alpha_1\alpha_2\dots\alpha_k}^m(t) \sum_{Y,\sigma} X_{\alpha_{k+1}|\dots|\alpha_n|Y[m^\sigma]} \right\}_\alpha. \quad (\text{III.44})$$

On the right side of (III.44) there are more types of Young tableaux than the one row tableau of the indices from the left side. This is a consequence of the nonlinearity of the system. To obtain a closed system of equations, though infinite, we must obtain the time evolution equation for  $X_{Y[m]}$  for any type of filled Young tableau  $Y[m]$ , not only for one row, as in (III.44). The equations written in the variables  $X_{Y[m]}$  will be bilinear, as desired; this procedure is known as Carleman bilinearization [47]. To obtain these equations, we need to introduce the sum of two filled Young tableaux. Let  $Y_1[m]$  and  $Y_2[\tilde{m}]$  be two filled Young tableaux with corresponding partitions  $N = \mu_1\lambda_1 + \mu_2\lambda_2 + \dots + \mu_k\lambda_k$  and  $\tilde{N} = \tilde{\mu}_1\tilde{\lambda}_1 + \tilde{\mu}_2\tilde{\lambda}_2 + \dots + \tilde{\mu}_k\tilde{\lambda}_k$ , respectively. We define their sum, denoted  $Y_1[m] \oplus Y_2[\tilde{m}]$ , by interlacing and ordering the rows of  $Y_1[m]$  and  $Y_2[\tilde{m}]$ . The sum corresponds to the partition  $N + \tilde{N} = \mu_1\lambda_1 + \mu_2\lambda_2 + \dots + \mu_k\lambda_k + \tilde{\mu}_1\tilde{\lambda}_1 + \tilde{\mu}_2\tilde{\lambda}_2 + \dots + \tilde{\mu}_k\tilde{\lambda}_k$ . For example:

$$\begin{array}{|c|c|c|c|} \hline 2 & 3 & 4 & 6 \\ \hline 5 & 7 & & \\ \hline 8 & 9 & & \\ \hline 1 & & & \\ \hline \end{array} \oplus \begin{array}{|c|c|c|c|c|} \hline 3 & 4 & 5 & 7 & 8 \\ \hline 1 & 2 & 10 & & \\ \hline 6 & 9 & & & \\ \hline & & & & \\ \hline \end{array} := \begin{array}{|c|c|c|c|c|} \hline 3 & 4 & 5 & 7 & 8 \\ \hline 2 & 3 & 4 & 6 & \\ \hline 1 & 2 & 10 & & \\ \hline 5 & 7 & & & \\ \hline 6 & 9 & & & \\ \hline 8 & 9 & & & \\ \hline 1 & & & & \\ \hline \end{array}$$

In other words,

$$X_{\begin{array}{|c|c|c|c|} \hline 2 & 3 & 4 & 6 \\ \hline 5 & 7 & & \\ \hline 8 & 9 & & \\ \hline 1 & & & \\ \hline \end{array}} \cdot X_{\begin{array}{|c|c|c|c|c|} \hline 3 & 4 & 5 & 7 & 8 \\ \hline 1 & 2 & 10 & & \\ \hline 6 & 9 & & & \\ \hline & & & & \\ \hline \end{array}} = X_{\begin{array}{|c|c|c|c|c|} \hline 3 & 4 & 5 & 7 & 8 \\ \hline 2 & 3 & 4 & 6 & \\ \hline 1 & 2 & 10 & & \\ \hline 5 & 7 & & & \\ \hline 6 & 9 & & & \\ \hline 8 & 9 & & & \\ \hline 1 & & & & \\ \hline \end{array}} = X_{\begin{array}{|c|c|c|c|} \hline 2 & 3 & 4 & 6 \\ \hline 5 & 7 & & \\ \hline 8 & 9 & & \\ \hline 1 & & & \\ \hline \end{array}} \oplus X_{\begin{array}{|c|c|c|c|c|} \hline 3 & 4 & 5 & 7 & 8 \\ \hline 1 & 2 & 10 & & \\ \hline 6 & 9 & & & \\ \hline & & & & \\ \hline \end{array}}$$

Using (III.44) and the definition of  $X_\Theta$  where  $\Theta$  is a filled Young tableau we obtain the equation of motion:

$$\dot{X}_\Theta = \sum_{i \in \text{Rows}(\Theta)} \left( \left\{ R_{\theta_1\theta_2\dots\theta_k}^m \sum_{|Y|=|m|} \sum_{\sigma \in S_{|Y|}/HY} X_{\theta_{k+1}|\dots|\theta_{n_i}|Y[m^\sigma] \oplus \widehat{\Theta}^i} \right\}_{\theta_1, \dots, \theta_{n_i}} \right) \quad (\text{III.45})$$

The rows of  $\Theta$  are indexed by  $i$  and the indices filling the row  $i$  are denoted by  $\theta_1 \dots \theta_{n_i}$ . The length of the row  $i$  of  $\Theta$  is  $n_i$ . Here, the summation by the tensor index  $m$  is understood. The hat above  $\Theta^i$  means that the row  $i$  was removed from  $\Theta$ . The brace indicates that we have to sum over all possible subsets  $(\theta_1 \theta_2 \dots \theta_k)$  of the set  $(\theta_1, \dots, \theta_{n_i})$ . The order of operations in the index of  $X$  in (III.45) is first concatenation  $|$  and then  $\oplus$ . An example of an equation of type (III.45) for the Michaelis-Menten system analyzed in a preceding section follows:

$$\begin{aligned} \dot{X}_{\begin{array}{|c|} \hline EE \\ \hline S \end{array}} &= -2k_1 X_{\begin{array}{|c|} \hline EEE \\ \hline S \end{array}} - 2k_1 X_{\begin{array}{|c|} \hline EE \\ \hline S \end{array}} - 2k_1 X_{\begin{array}{|c|} \hline ES \\ \hline S \end{array}} - 2k_{-2} X_{\begin{array}{|c|} \hline EEP \\ \hline S \end{array}} - 2k_{-2} X_{\begin{array}{|c|} \hline EE \\ \hline P \end{array}} - 2k_{-2} X_{\begin{array}{|c|} \hline EP \\ \hline S \end{array}} \\ &\quad - k_1 X_{\begin{array}{|c|} \hline EE \\ \hline S \end{array}} - k_1 X_{\begin{array}{|c|} \hline EE \\ \hline S \end{array}} + 2k_{-1} X_{\begin{array}{|c|} \hline EC \\ \hline S \end{array}} + 2k_2 X_{\begin{array}{|c|} \hline EC \\ \hline S \end{array}} - 2\gamma_E X_{\begin{array}{|c|} \hline EE \\ \hline S \end{array}} - \gamma_S X_{\begin{array}{|c|} \hline EE \\ \hline S \end{array}} + k_{-1} X_{\begin{array}{|c|} \hline EE \\ \hline C \end{array}} \\ &\quad + k_S X_{\begin{array}{|c|} \hline EE \\ \hline \end{array}} \end{aligned}$$

The terms on the right side of the above formula were obtained from (III.45). For example, for  $i = \begin{array}{|c|} \hline EE \\ \hline \end{array}$ ,  $m = EP$ ,  $|Y| = 2$ , we have

$$\begin{aligned} -2k_{-2} X_{\begin{array}{|c|} \hline EEP \\ \hline S \end{array}} &= R_E^{EP} X_{E | \begin{array}{|c|} \hline EP \\ \hline S \end{array}} \oplus \begin{array}{|c|} \hline S \\ \hline \end{array} \\ -2k_{-2} X_{\begin{array}{|c|} \hline EE \\ \hline P \end{array}} - 2k_{-2} X_{\begin{array}{|c|} \hline EP \\ \hline S \end{array}} &= R_E^{EP} X_{E | \begin{array}{|c|} \hline EP \\ \hline \end{array}} \oplus \begin{array}{|c|} \hline S \\ \hline \end{array} \end{aligned}$$

### C. Equation of Motion for Rational Transition Probabilities

The Master Equation is now

$$\frac{\partial P(q, t)}{\partial t} = \sum_{\epsilon} \frac{f_{\epsilon}(q - \epsilon, t)}{\tilde{f}_{\epsilon}(q - \epsilon, t)} P(q - \epsilon, t) - \sum_{\epsilon} \frac{f_{\epsilon}(q, t)}{\tilde{f}_{\epsilon}(q, t)} P(q, t), \quad (\text{III.46})$$

where  $f(q, t)$  and  $\tilde{f}(q, t)$  are polynomial functions in the state variable  $q$ .

Multiplying both sides of (III.46) with  $h(q, t) = \prod_{\epsilon} \tilde{f}_{\epsilon}(q, t) \tilde{f}_{\epsilon}(q - \epsilon, t)$  produces a Master Equation with polynomial coefficients:

$$h(q, t) \frac{\partial P(q, t)}{\partial t} = \sum_{\epsilon} T_{\epsilon}^{(1)}(q - \epsilon, t) P(q - \epsilon, t) - \sum_{\epsilon} T_{\epsilon}^{(2)}(q, t) P(q, t). \quad (\text{III.47})$$

The decomposition in the factorial base will be

$$h(q, t) = \sum_m M^m(t) \mathbf{e}_{\bar{m}}(q) \quad (\text{III.48})$$

$$T_{\epsilon}^1(q, t) = \sum_{m_1} M_{\epsilon}^{m_1}(t) \mathbf{e}_{\bar{m}_1}(q) \quad (\text{III.49})$$

$$T_{\epsilon}^2(q, t) = \sum_{m_2} M_{\epsilon}^{m_2}(t) \mathbf{e}_{\bar{m}_2}(q) \quad (\text{III.50})$$

The boundary condition  $m \geq -\epsilon$  that applies to  $f_\epsilon(q, t)$  also applies to  $T_\epsilon^1(q, t)$  and  $T_\epsilon^2(q, t)$  and thus the equation for  $F(z, t)$  is

$$\sum_{\epsilon} M_{\epsilon}^m(t) z^{\bar{m}} \partial_m \partial_t F = \sum_{\epsilon} M_{\epsilon}^{m_1}(t) z^{\epsilon + \bar{m}_1} \partial_{m_1} F - \sum_{\epsilon} M_{\epsilon}^{m_2}(t) z^{\bar{m}_2} \partial_{m_2} F \quad (\text{III.51})$$

Change the variable to  $F(z, t) = e^{X(z, t)}$ .

$$\begin{aligned} & \sum_{\epsilon} M_{\epsilon}^m(t) z^{\bar{m}} \left( \sum_{Y, \sigma} \partial_{Y[m\sigma]} \dot{X}(z, t) + \dot{X}(z, t) \sum_{Y, \sigma} \partial_{Y[m\sigma]} X(z, t) \right) = \\ & \sum_{\epsilon} M_{\epsilon}^{m_1}(t) z^{\epsilon + \bar{m}_1} \sum_{Y_1, \sigma_1} \partial_{Y_1[m_1\sigma_1]} X(z, t) - \sum_{\epsilon} M_{\epsilon}^{m_2}(t) z^{\bar{m}_2} \sum_{Y_2, \sigma_2} \partial_{Y_2[m_2\sigma_2]} X(z, t) \end{aligned} \quad (\text{III.52})$$

Take the partial derivative of (III.52) with respect to the tensor index  $\alpha_1 \dots \alpha_n$  using the general formula

$$\partial_{\alpha_1 \dots \alpha_n} (fgh) = \left\{ \partial_{\alpha_1 \dots \alpha_{k_1}} f \partial_{\alpha_{k_1+1} \dots \alpha_{k_2}} g \partial_{\alpha_{k_2+1} \dots \alpha_n} h \right\}_{\alpha}. \quad (\text{III.53})$$

The braces indicates the summation for all triplets of disjoint sets  $(\alpha_1 \dots \alpha_{k_1})$ ,  $(\alpha_{k_1+1} \dots \alpha_{k_2})$  and  $(\alpha_{k_2+1} \dots \alpha_n)$  that form a partition of the tensor index  $\alpha_1 \dots \alpha_n$ .

The time evolution equation for the factorial cumulants is then

$$\begin{aligned} & \left\{ Q_{\alpha_1 \dots \alpha_k}(\bar{m}) \dot{X}_{\alpha_{k+1} | \dots \alpha_n | Y[m\sigma]} + Q_{\alpha_1 \dots \alpha_{k_1}}(\bar{m}) \dot{X}_{\alpha_{k_1+1} | \dots \alpha_{k_2} | Y[m\sigma]} X_{\alpha_{k_2+1} | \dots \alpha_n | Y[m\sigma]} \right\}_{\alpha} = \\ & \left\{ M_{\epsilon}^{m_1}(t) Q_{\alpha_1 \dots \alpha_k}(\epsilon + \bar{m}_1) X_{\alpha_{k+1} | \dots \alpha_n | Y_1[m_1\sigma_1]} - M_{\epsilon}^{m_2}(t) Q_{\alpha_1 \dots \alpha_k}(\bar{m}_2) X_{\alpha_{k+1} | \dots \alpha_n | Y_2[m_2\sigma_2]} \right\}_{\alpha} \end{aligned} \quad (\text{III.54})$$

where summation over the dummy indices  $m$ ,  $m_1$  and  $m_2$  is implied. This equation was used to solve the Hill feedback control (II.18). Instead of the Carleman bilinearization, which is difficult to apply for this case, we can use the variational approach [47] and (II.21, II.22).

#### IV. DISCUSSION

In this work, we have extended the analysis carried out in [30] from linear to nonlinear stochastic networks. The genetic regulatory networks are stimulated by a set of signal generators. In an experimental setting, a specific set of molecules (mRNAs, proteins) are selected and their time variation is controlled by input signal generators. As a consequence, the number of the different molecules that comprise the genetic regulatory network will vary in time. The time variation of these molecular numbers is subject to a system of equations. We deduce this system of equations for a stochastic genetic regulatory network described by a *state*, a set of *transitions* and their *transition probabilities*. The nonlinear effects are due to the transition probabilities being polynomial or rational functions in the state components. The system being stochastic, the variables of interest are the mean and the correlations for the molecular species which comprise the genetic network.

The time dependence of these means and correlations are expressed in terms of a set of factorial cumulants. The network's dynamic is described by the time variation of these factorial cumulants. The time evolution equations take the form (III.44) for polynomial transition probabilities and (III.54) for rational transition probabilities.

We solved the equation of motion for four genetic regulatory networks.

The first example aims to further generalize the results of [30]. There, a linear stochastic genetic network was analyzed and the equations for the factorial cumulants up to order two were solved. In the present paper, we study a nonlinear connection of two linear systems. We arrived at the conclusion that the solution to the nonlinear coupled systems implies factorial cumulants of order more than two. The equations for the cumulants of a linear network can be organized in an hierarchical structure with respect to the order of the cumulants, see Fig. 3 System 1. The cumulants up to a given order form a closed system of equations, which is not the case for a typical nonlinear network. However, we also have shown that for the special case of linear systems, that nonlinear coupling does not require an infinite system of equations. Indeed, if we need to solve for the second order factorial cumulants for System 2, then we need up to fourth order cumulants for System 1.

The second example uses the equations (III.54) to study an autoregulatory system that is frequently used to explain experimental results. The system is composed of one gene which regulates its own transcription. The protein acts on mRNA production through a term that is a rational function in protein number, see Table 2. We studied this system from a synthetic biology perspective, aiming to design a logic gate. The biomolecular device being intrinsically probabilistic, a logic 1 will be characterized by a mean value and a standard deviation from the mean; similar for the logic 0. The distance between the mean values of the logical levels should be sufficiently large to include the standard deviations of both logic levels. We presented a scheme to design a logic gate from an autoregulatory gene, see Fig. 7. From another point of view, the autoregulatory system is useful for checking the effectiveness of the factorial cumulants. Namely, the analytical solutions must match the results from a Monte Carlo simulation. Such a comparison was done for the case when the signal generator is closed, causing the gene transcription to be completely under the control of its protein product. Because inside a living cell many regulatory proteins appear in small number, we choose the network parameters so that the mRNA number fluctuates around 12 molecules, Table 3. We found that the traditional mass action equations (II.25) do not explain the Monte Carlo simulations; to explain the simulated results we had to use equations that involve higher order factorial cumulants. Next, we study the response of the system to a time variable signal generator. The input-output relations for protein are presented in terms of the Laplace transforms of the time dependent variables (II.30).

The stochastic version of the classical Michaelis-Menten mechanism for enzymic catalysis is the subject of the third example. An input signal generator acting on the enzyme will drive the source, complex and product. The time variation of these molecules is described by the system of equations (II.31). For an oscillatory signal generator, the Michaelis-Menten process behaves as a molecular amplifier. Namely, it is possible to drive large oscillations in the product P using small oscillations in the enzyme E, Fig. 12. Another aspect that we investigated for this process is its transitory regime, Fig. 13. We showed that the dynamical equations (II.31) and the Monte Carlo simulations agree with each other. Thus, we can use the dynamical equations to produce the statistical variables, rather than generating many instances of the stochastic process.

The last example is based on E2F1 regulatory element. The transcription is controlled by three transcription factors: E2F1, DP1 and pRb. Here we studied the interference of three signal generators. Each generator will modulate the mRNA production as is specified by the transfer functions from (II.37). The E2F1 regulatory element, as was studied here, is a part of a complex system of

many transcription factors. If we see the E2F1 as a module in a complex system, than we have to interconnect many modules to obtain the whole complex system. How to decompose a complex system into its modules and how to interconnect many modules to obtain a complex system is left for a future study. The dynamical equations for all these examples of gene regulatory networks are special cases of a general system of equations that were obtained in the last two sections of the article. For transition probabilities that are polynomial in the state components, the system of equations is (III.44). This system of equations is polynomial in the  $X_m$  variables. With the Carleman bilinearization method, the system is transformed into (III.45). Filled Young tableaux that appear in (III.45) help to construct new variables from the products of the  $X_m$  variables. For rational transition probabilities, the equation is (III.54) and was used to solve the Hill feedback control (II.18).

The procedure outline above can be applied to many other genetic networks such as networks with multistable steady states [21]. The simplest network from this class is bistable; it toggles between two stable steady states. Biological examples of bistable systems include the lambda lysis-lysogeny switch and the hysteretic lac repressor system. Another avenue of research is to understand the feedback theory in terms of factorial cumulants. Negative feedback stabilizes the system whereas positive feedback is responsible for oscillations and multistable states. The feedback design principles are important in developing biomolecular devices. The question is thus: How to translate the feedback design theory from the classical control theory into the language of nonlinear stochastic genetic networks? The control theory for nonlinear stochastic genetic networks should also contain studies about observability and reachability. From another perspective, studies on the factorial cumulants discard will be important. What is the minimum cummulat order we need to retain to reach a predefined precision for the output variables?

From an experimental point of view, practical implementation of signal generators, on both the mRNA and protein level, will boost research on cell signaling. Experimentally it was proven that a source of oscillations propagates into a genetic network. Namely, in [48] a group of mice were exposed for 2 weeks to an external source of 12 hours light followed by 12 hours of darkness. This input external oscillator entrained the internal clock of the cell. The output signals (mRNA expression levels) were measured by sacrificing a mouse from the entrained group every 4 hours for 2 days. The mice were kept in compete darkness during the 2 days measurement period, so only the internal clock will affect the mRNA levels. The data, collected with an Affymetrix (Santa Clara, CA) platform, showed that form  $\approx 6000$  expressed genes,  $\approx 500$  oscillated with a 24-h period. The next experiment would be to implement the light switch from Fig. 2, and drive one of the core component of the clock mechanism directly from its promoter. Then use a microarray experiment to measure the mRNA levels and find the set of genes that follow the frequency of signal generator. Besides a microarray design, which screen large sets of genes at few time points, an experimental design based on a phototube, [49], can record the expression of few genes but in real time. Thus detailed information about the time variation of specific genes can be recorded. Such detailed information is crucial for developing a proper mathematical description of gene interaction. Models developed in the field of system identification [50], in conjunction with the approach presented in this article, will help to better interpretate the measured data. With an input signal generator that acts on a target gene or protein, we can also measure the speed of propagation of the signal through the gene network. The speed of propagation can be very fast; for example the G protein-coupled receptor switches in milliseconds, [51]. To conclude, understanding how the behavior of living cells emerges from a genetic network, experimental designs should be correlated with mathematical theories. We hope that the methods presented in this article will help to create new experimental designs for systems biology.



## V. MATERIALS AND METHODS

### A. Monte Carlo Simulations for Time Dependent Transition Probabilities

The time dependent Direct Gillespie algorithm was used to generate the stochastic simulations [35]. We present here the Gillespie algorithm using the notations introduced before.

We denote by  $p_\epsilon(\tau | q, t)d\tau$  the probability that the system will jump in direction  $\epsilon$  in the time interval  $[t + \tau, t + \tau + d\tau]$  if it stayed in the state  $q$  in the time interval  $[t, t + \tau]$ . In terms of transition probabilities:

$$p_\epsilon(\tau | q, t)d\tau = e^{-\sum_\eta \int_0^\tau T_\eta(q, t+\tau')d\tau'} T_\epsilon(q, t + \tau)d\tau \quad (\text{V.1})$$

where  $T_\epsilon(q, t + \tau)d\tau$  is the probability that the system will jump from the state  $q$  in direction  $\epsilon$  in the time interval  $[t + \tau, t + \tau + d\tau]$ , regardless of the system's history before  $t + \tau$ . The other term of (V.1)

$$e^{-\sum_\eta \int_0^\tau T_\eta(q, t+\tau')d\tau'} \quad (\text{V.2})$$

is the probability that the system will stay in the state  $q$  in the time interval  $(t, t + \tau)$ .

To obtain (V.2) divide the interval  $(t, t + \tau)$  in small pieces  $(t + k\delta, t + (k + 1)\delta)$  for  $k = 0, \dots, N - 1$ , with  $N\delta = \tau$ . Then the probability that the system will stay in the state  $q$  in the time interval  $(t, t + \tau)$  is the product of the probabilities that the system will stay in the state  $q$  in the intervals  $(t + k\delta, t + (k + 1)\delta)$ . Because  $\delta$  is small we can use the definition of the transition probability to find that  $1 - \sum_\eta T_\eta(q, t + k\delta)\delta$  is the probability that the system will stay in the state  $q$  in the time interval  $(t + k\delta, t + (k + 1)\delta)$ . The fact that  $\delta$  is small makes also possible to bring this probability into an exponential form

$$e^{-\int_{k\delta}^{(k+1)\delta} \sum_\eta T_\eta(q, t+\tau')d\tau'} \quad (\text{V.3})$$

The exponential form will help to transform the product of the probabilities into a sum. Multiplying (V.3) for  $k = 1, \dots, N - 1$  we obtain  $e^{-\sum_\eta \int_0^\tau T_\eta(q, t+\tau')d\tau'}$ , which appear in the right side of (V.1).

The cumulative distribution function of  $p_\epsilon(\tau | q, t)d\tau$  is

$$\begin{aligned} F(\tau | q, t) &= \int_0^\tau \sum_\epsilon p_\epsilon(\tau'' | q, t)d\tau'' \\ &= \int_0^\tau \sum_\epsilon e^{-\sum_\eta \int_0^{\tau''} T_\eta(q, t+\tau')d\tau'} T_\epsilon(q, t + \tau'')d\tau'' \\ &= 1 - e^{-\int_0^\tau \sum_\epsilon T_\epsilon(q, t+\tau')d\tau'} \end{aligned}$$

After the transition took place at time  $t$ , the next transition will take place at  $t + \tau$ , with  $\tau$  a solution of the equation  $F(\tau | q, t) = U_1$ . Here  $U_1$  is a uniform random number from  $[0, 1]$  and  $q$  and

$t$  are known. We will find  $\tau$  using the bisection method [52]. The root is bracketed in the interval  $[-\ln(1 - U_1)M(q)^{-1}, -\ln(1 - U_1)m(q)^{-1}]$ , where

$$m(q) = \inf_{x \in \mathbf{R}} \sum_{\epsilon} T_{\epsilon}(q, x), \quad (\text{V.4})$$

$$M(q) = \sup_{x \in \mathbf{R}} \sum_{\epsilon} T_{\epsilon}(q, x), \quad (\text{V.5})$$

and the procedure is stopped when an accuracy of  $10^{-\alpha}$  is reached. We used  $\alpha = 5$ .

After  $\tau$  was found, a second random number  $U_2$  is necessary to find which transition will take place. In other words, we have to find one  $\epsilon_{\mu}$  from all possible transitions  $\mu = 1 \dots \Upsilon$ . The unknown  $\mu$  from the set of indices  $1, \dots, \Upsilon$  is obtained from

$$\sum_{k=1}^{\mu-1} T_{\epsilon_k}(q, t + \tau) \leq U_2 \sum_{k=1}^{\Upsilon} T_{\epsilon_k}(q, t + \tau) \leq \sum_{k=1}^{\mu} T_{\epsilon_k}(q, t + \tau).$$

Analytical computations and numerical analysis were done with Maple (Waterloo Maple Inc., Waterloo, Ontario, Canada) and Matlab (Mathworks, Natick, Massachusetts, United States).

## VI. ACKNOWLEDGMENTS

O. Lipan is grateful to Wing H. Wong for his initial impulse for writing this article, continuous encouragements and critical inputs. We thank our colleagues at the Center for Biotechnology and Genomic Medicine for their support. The paper was supported by O. Lipan startup package for which we thank the Medical College of Georgia and the Center for Biotechnology and Genomic Medicine.

- 
- [1] Lipan O, Achimescu S (2005) Modulation of nonlinear stochastic gene regulatory network by input signals. Poster at the 3rd International Conference on Pathways, Networks, and Systems: Theory and Experiments, October 2-7, Rhodes Greece.
  - [2] Levine M, Davidson EH (2005) Gene regulatory networks for development. *Proc Natl. Acad. Sci. USA* 102 (14): 4936 – 4942.
  - [3] Westerhoff HV, Palsson BO (2004) The evolution of molecular biology into systems biology. *Nature Biotechnology* V. 22 N.10: 1249 – 1252.
  - [4] Hood L, Perlmutter PM (2004) The impact of systems approaches on biological problems in drug discovery. *Nature Biotechnology* V. 22 N.10: 1215 – 1217.
  - [5] Ehrenberg M, Elf J, Aurell E, Sandberg E, Tegnér J (2003) Systems biology is taking off. *Genome Research* 13(11): 2377 – 2380.
  - [6] Ozbudak EM, Thattai M, Kurtser I, Grossman AD, van Oudenaarden A (2002) Regulation of noise in the expression of a single gene. *Nature Genetics* 31: 69 – 73.
  - [7] Basu S, Mehreja R, Thiberge S, Chen MT, Weiss R (2004) Spatiotemporal control of gene expression with pulse generating networks. *Proc Natl. Acad. Sci. USA* 101: 6355 – 6360.
  - [8] Mangan S, Zaslaver A, Alon U (2003) The coherent feedforward loop serves as a sign-sensitive delay element in transcription networks. *JMB Vol* 334/2: 197 – 204.

- [9] Gardner TS, di Bernardo D, Lorenz D, Collins JJ (2003) Inferring genetic networks and identifying compound mode of action via expression profiling. *Science* 301: 102 – 105.
- [10] Hasty J, Dolnik M, Rottschäfer V, Collins JJ (2002) A synthetic gene network for entraining and amplifying cellular oscillations. *Phys. Rev. Lett.* 88 (14), art. no. 148101: 1 – 4.
- [11] Hao N, Yildirim N, Wang Y, Elston TC, Dohlman HG (2003) Regulators of G protein signaling and transient activation of signaling: experimental and computational analysis reveals negative and positive feedback controls on G protein activity. *Journal of Biological Chemistry* 278: 46506 – 46515.
- [12] Becskei A, Serrano L (2000) Engineering stability in gene networks by autoregulation. *Nature* 405: 590 – 593.
- [13] Brent R (2004) A partnership between biology and engineering. *Nature* 22: 1211 – 1214.
- [14] Arkin AP (2001) Synthetic cell biology. *Current Opinion in Biotechnology* 12: 638 – 644.
- [15] Endy D, Brent R (2001) Modelling cellular behaviour. *Nature* 409:391 – 395.
- [16] Alon U (2003) Biological Networks: The tinkerer as an engineer. *Science* 301: 1866 – 1867.
- [17] Guet C, Elowitz MB, Hsing W, Leibler S (2002) Combinatorial synthesis of genetic networks. *Science* 296(5572): 1466 – 1470.
- [18] Beuter A, Glass L, Mackey MC, Titcombe MS(Editors) (2003) Nonlinear dynamics in physiology and medicine. *Interdisciplinary Applied Mathematics*, vol. 25, Springer-Verlag, New York. 434 p.
- [19] May MR (2004) Uses and abuses of mathematics in biology. *Science* V303: 790 – 793.
- [20] van Kampen NG (1992) *Stochastic Processes in Physics and Chemistry*. NorthHolland, Amsterdam. 465 p.
- [21] Ozbudak EM, Thattai M, Lim HN, Shraiman BI, van Oudenaarden A (2004) Multistability in the lactose utilization network of *Escherichia coli*. *Nature* 427(6976): 737 – 40.
- [22] Arkin A, Ross J, McAdams HH (1998) Stochastic kinetic analysis of developmental pathway bifurcation in phage  $\lambda$ -infected *Escherichia coli* cells. *Genetics* 149: 16331648.
- [23] Pedraza JM, van Oudenaarden A (2005) Noise propagation in gene networks. *Science* 307: 1965 – 1969.
- [24] Rao CV, Wolf DM, Arkin AP (2002) Control, exploitation and tolerance of intracellular noise. *Nature* 420: 231 – 237.
- [25] Elf J, Ehrenberg M (2003) Fast evaluation of fluctuations in biochemical networks with the linear noise approximation. *Genome Research* 13: 2475 – 2484.
- [26] Paulsson J (2004) Summing up the noise in gene networks. *Nature*.29;427(6973):415 – 418.
- [27] Berg OG (1978) A model for the statistical fluctuations of protein numbers in a microbial population. *J. Theor. Biol.* 71: 587 – 603.
- [28] Thattai M, van Oudenaarden A, (2001) Intrinsic noise in gene regulatory networks. *Proc. Natl. Acad. Sci. USA* 98: 8614 – 8619.
- [29] Swain PS, Elowitz MB, Siggia ED (2002) Intrinsic and extrinsic contributions to stochasticity in gene expression. *Proc. Natl. Acad. Sci. USA* 99: 12795 – 12800.
- [30] Lipan O, Wong WH, The use of oscillatory signals in the study of genetic networks. *Proc. Natl. Acad. Sci. USA*. 102: 7063 – 7068.
- [31] Gadgil C, Lee CH, Othmer HG (2005) A stochastic analysis of first-order reaction networks. *Bull. Math. Biol.* In press.
- [32] Samoilov M, Arkin A, Ross J (2002) Signal processing by simple chemical systems. *J. Phys. Chem. A* 106: 10205 – 10221.
- [33] Khalil H (1996) *Nonlinear Systems*. Prentice Hall, Inc.. 765 p.
- [34] Shimizu-Sato S, Huq E, Tepperman JM, Quail, PH (2002) A light-switchable gene promoter system. *Nature Biotechnology* 20: 1041 – 1044.
- [35] Gillespie DT (1992) *Markov processes: An introduction for physical scientists*. Academic Press, San Diego. 565 p.
- [36] McCullagh P (1987) *Tensor methods in statistics. Monographs in statistics and applied probability*. Chapman and Hall, Cambridge, England. 285p.
- [37] Kitano H (2003) A graphical notation for biochemical networks. *Biosiloco*, Vol.1 ,No. 5: 169 – 176.
- [38] Lee TI, Rinaldi NJ, Robert F, Odom DT, Bar-Joseph Z, et al. (2002) Transcriptional regulatory networks in *Saccharomyces cerevisiae*. *Science* 298: 799 – 804.
- [39] Elowitz MB, Leibler S (2000) A synthetic oscillatory network of transcriptional regulators. *Nature* 403: 335 – 338.

- [40] Tzafriria AR, Edelmana ER, (2004) The total quasi-steady-state approximation is valid for reversible enzyme kinetics. *Journal of Theoretical Biology* 226: 303313.
- [41] Muller H, Helin K. (2000) The E2F transcription factors: key regulators of cell proliferation. *Biochim. Biophys. Acta* 1470: M1-M12.
- [42] Phillips AC, Vousden KH (2001) E2F-1 induced apoptosis. *Apoptosis* 6: 173 – 182.
- [43] Kohn KW (1999) Molecular interaction map of the mammalian cell cycle control and DNA repair systems. *Molec. Biol. Cell* 10(8): 2703 – 2734.
- [44] Sturmfels B (2002) Solving systems of polynomial equations. AMS, CBMS Number 97. 152 p.
- [45] Mohler RR (1991) Nonlinear systems vol.2. Applications to bilinear control. Prentice Hall, Inc.. 213 p.
- [46] Constantine GM, Savits TH (1996) A multivariate Faà di Bruno formula with applications. *Trans. Amer. Math. Soc.* 348, no. 2: 503 – 520.
- [47] Rugh W (1981) Nonlinear system theory. The Volterra/Wiener approach. Johns Hopkins University Press. 330 p.
- [48] Storch KF, Lipan O, Leykin I, Viswanathan N, Davis FC (2002) Extensive and divergent circadian gene expression in liver and heart. *Nature* 417: 78 – 83.
- [49] Izumo M, Johnson CH, Yamazaki S (2003) Circadian gene expression in mammalian fibroblasts revealed by real-time luminescence reporting: Temperature compensation and damping. *Proc. Natl. Acad. Sci. USA* 100: 16089 – 16094.
- [50] Ljung L (1999) System identification - Theory for the user. 2nd edition. Prentice Hall, Inc.. 603 p.
- [51] Vilardaga JP, Bünemann M, Krasel C, Castro M, Lohse MJ (2003) Measurement of the millisecond activation switch of G protein-coupled receptors in living cells. *Nature Biotechnology* 21: 807 – 812.
- [52] Press WH, Flannery BP, Teukolsky SA, Vetterling WT (1992) Numerical recipes in C: The art of scientific computing. Cambridge University Press. 994 p.